

2017

# The effect of phosphorus and nitrogen limitation on viral infection in microcystis aeruginosa NIES298 using the cyanophage Ma-LMM01

Katelyn McKindles

Follow this and additional works at: <http://commons.emich.edu/theses>



Part of the [Biology Commons](#)

---

## Recommended Citation

McKindles, Katelyn, "The effect of phosphorus and nitrogen limitation on viral infection in microcystis aeruginosa NIES298 using the cyanophage Ma-LMM01" (2017). *Master's Theses and Doctoral Dissertations*. 741.  
<http://commons.emich.edu/theses/741>

This Open Access Thesis is brought to you for free and open access by the Master's Theses, and Doctoral Dissertations, and Graduate Capstone Projects at DigitalCommons@EMU. It has been accepted for inclusion in Master's Theses and Doctoral Dissertations by an authorized administrator of DigitalCommons@EMU. For more information, please contact [lib-ir@emich.edu](mailto:lib-ir@emich.edu).

The Effect of Phosphorus and Nitrogen Limitation on Viral Infection in  
*Microcystis aeruginosa* NIES298 using the Cyanophage Ma-LMM01

by

Katelyn McKindles

Thesis

Submitted to the Department of Biology

Eastern Michigan University

in partial fulfillment of the requirements

for the degree of

MASTER OF SCIENCE

in

Cell and Molecular Biology

Thesis Committee:

Michael Angell, Ph.D. Chair

Daniel Clemans, Ph.D.

Steven Francoeur, Ph.D.

David Kass, Ph.D.

July 20, 2017

Ypsilanti, Michigan

## Acknowledgments

First, I want to thank my advisor, Dr. Michael Angell of Eastern Michigan University, for allowing me to develop this project from scratch, which was in a field new to him, and I want to thank him for the time and energy that he contributed towards the project's development. He consistently allowed this paper to be my own work but steered me in the right the direction whenever he thought I needed it.

I would also like to thank Dr. Takashi Yoshida of Kyoto University for his generous donation of the cyanophage, Ma-LMM01, and Dr. Tim Davis of the NOAA Great Lakes Environment Research Laboratory for his generous donation of the North American stains of *M. aeruginosa*, all used in this study. Without these donations, this project would not be possible.

I also want to thank Dr. Steven Francoeur, who was a large help in both the cyanobacterial biology and statistical aspect of the project, and my other committee members, Dr. Daniel Clemans and Dr. David Kass, for their guidance in navigating the end of my master's career.

Finally, I must express my very profound gratitude to my family, to my many friends who are on similar journeys in life, and to my boyfriend for providing me with unfailing support and continuous encouragement throughout my years of study and through the process of researching and writing this thesis. This accomplishment would not have been possible without them.

Thank you.

## Abstract

Throughout different times in freshwater cyanobacterial harmful algal blooms (cHAB), the availability of specific nutrients from the environment varies, causing fluctuations in the severity and species composition of a bloom. In addition to nutrient regulation of blooms, the cyanobacteria are subject to regulation by biotic factors, including phage infection. To address the potential role of cyanophages on the dominant species in most cHABs during nutrient-limited periods, we studied a specific host-phage system: Ma-LMM01 (phage) and *Microcystis aeruginosa* strain NIES298 (host), both of which originate from a eutrophic lake in Japan. The effect of phosphate and nitrogen limitation on phage and host replication was evaluated through modification of *M. aeruginosa* culture media. Growth of the host cells was monitored by culture light absorbance at 600 nm, while phage (genome) replication was quantified using real-time quantitative PCR (qPCR). Under phosphorus-limited conditions, Ma-LMM01 infected cells demonstrated a decrease in growth rate and carrying capacity compared to uninfected and infected non-limited cultures. This relationship suggests that phage infection decreases *M. aeruginosa* growth to a greater degree under phosphorous stress than when the nutrient is readily available. In this model, these results indicate cyanophage replication may accelerate cHAB collapse under phosphorus-limiting conditions, and that increased concentrations of phosphorus may decrease the impact of cyanophage infections in the wild.

## Table of Contents

Acknowledgments .....	ii
Abstract .....	iii
List of Tables .....	v
List of Figures .....	vi
Introduction .....	1
Materials and Methods .....	9
2.1 Cell Culture and Maintenance .....	9
2.2 Growth Quantitation of <i>Microcystis aeruginosa</i> .....	11
2.3 DNA Extraction and Quantitative Polymerase Chain Reaction (qPCR) .....	11
2.4 Strain Identification using Restriction Digest Profiles .....	14
2.5 Viral Infection .....	15
2.5.1 Characterization of Viral Infection .....	15
2.5.2 Limited Phosphorus and Nitrogen Infection, Trial 1 .....	16
2.5.3 Limited Phosphorus and Nitrogen Infection, Trial 2 .....	17
2.5.4 Phosphorus Limited Trial .....	18
2.6 Statistical Analysis .....	19
Results .....	20
3.1 Growth Quantitation of <i>Microcystis aeruginosa</i> .....	20
3.2 Strain Identification using Restriction Digest Profiles .....	21
3.3 Presence of Viral Genes in <i>M. aeruginosa</i> Genomes, Pre-Infection .....	23
3.4 Characterization of Viral Infection .....	24
3.5 Host Specificity Test .....	27
3.6 Nutrient Stress Infection Trials .....	29
Discussion .....	39
4.1 Characterization of Viral Infection in NIES298 .....	39
4.2 Testing for North American Strains of <i>M. aeruginosa</i> for Ma-LMM01 Susceptibility .....	43
4.3 Combined Effect of Nitrogen Limitation and Viral Infection .....	45
4.4 Combined Effect of Phosphorus Limitation and Viral Infection .....	47
Conclusion .....	53
Literature Cited .....	55

## List of Tables

Table 1. <i>Microcystis aeruginosa</i> strains and the cyanophage used in this study, including the location of origin and toxin producing ability. ....	10
Table 2. List of DNA primers for qPCR used in this study. ....	13
Table 3. Potential restriction enzyme and gene combinations to create a restriction digest profile. ....	14
Table 4. Modifications of CB media to assess the impact of nutrient conditions on phage infection .....	18
Table 5. Summary of molecular profiles of the strains of <i>Microcystis aeruginosa</i> used in this project.....	23

## List of Figures

Figure 1. Flow chart of the relative viral genome replication methodology used in this study. _____	13
Figure 2. General outline of the methodology used in the nutrient-modified infection trials. _____	17
Figure 3. Growth Curve of <i>M. aeruginosa</i> using UV/Vis Spectrophotometry. _____	20
Figure 4. Growth of <i>Microcystis aeruginosa</i> NIES298 using UV/Vis Spectrophotometry and manual cell counts. _____	21
Figure 5. Strain Identification based on Restriction Digests of the Amplified Cyanobacterial genes analyzed on 2% Agarose Gel. _____	22
Figure 6. Initial analysis of phage genes g91 and nblA prior to infection, analyzed on a 2% agarose gel. _____	24
Figure 7. Verification of an infection in <i>M. aeruginosa</i> NIES298. _____	26
Figure 8. Host specificity test of Ma-LMM01 on North American Strains of <i>Microcystis aeruginosa</i> CPCC124, LB2385, and LB2386. _____	28
Figure 9. Trial 1: Infection in replete media and transfer into nutrient limited media. _____	31
Figure 10. Trial 1: Growth rate and carrying capacity of each media. _____	33
Figure 11. Trial 2: Infection in nutrient limited media. _____	35
Figure 12. Trial 3: Infection in phosphorus limited media and phosphorus limited media with salt compensation. _____	38

## **Introduction**

Cyanobacteria are a diverse group of microorganisms that are important to the environment as they are obligate photoautotrophs, some with the capability to fix atmospheric nitrogen, store phosphorus, and sequester iron and other trace metals (Deng and Hayes 2008; Paerl and Otten 2013). Cyanobacterial harmful algal blooms (cHABs) are caused when there is a sharp increase in growth of these microscopic algae, often resulting in water color changes based on the pigmentation of the main species in the bloom (Gilbert et al. 2005). These cHABs can cause many problems: increased biomass can lead to the death of lake wildlife through oxygen depletion and by blocking sunlight penetration through the water column (Lopez et al. 2008), and some cyanobacterial species have the capability to create chemically stable monocyclic heptapeptide toxins, known as microcystins (Paerl and Otten 2013).

The formation of cHABs is not only an environmental concern, but an economic concern as well. Lake Erie is a local freshwater environment with large cHABs that can prevent use of the lake for recreation purposes such as boating and fishing. Additionally, a cHAB in the western basin of Lake Erie in 2011 (a record breaking year) shut down the water supply for the city of Toledo, Ohio, and surrounding areas (Michalak et al. 2013). Due to the harmful nature of these blooms, and the money required to clean them up, there is a need for research on regulation of cHABs and methods for controlling them (Lopez et al. 2008). Understanding how external factors can shorten or lengthen the viability of the bloom is vital for establishing methods to control them.



*Microcystis aeruginosa* is a cyanobacterium that is frequently found in freshwater cHABs (Paerl and Otten 2013; Lopez et al. 2008), which occur world-wide, including the Laurentian lower Great Lakes and several lakes in Japan, Canada, Australia, China, and Europe (Davis et al. 2014). *Microcystis aeruginosa* is a gram-negative coccus that forms colonies on the surface of the water (in the form of mats) in the wild and has a large gas vesicle to help maintain buoyancy (Mlouka et al. 2004). Some members of this species are equipped with a series of genes that allow for the production of microcystins (*mcy* genes) and other toxins. Microcystin-LR (MC-LR) is particularly known to affect the liver and promote tumor formation if consumed, and it can kill livestock, pets, and humans exposed to contaminated water (Butler et al. 2009). This compound accumulates inside the bacterium, is released upon cellular death, and is particularly dangerous after the formation of cHABs due to the high concentration of the toxin-producing microbes. MC-LR can have different effects on an individual depending on the amount of exposure. Acute toxicity has been linked with nausea and vomiting, weakness, gastroenteritis, and acute liver failure through hepatic necrosis (Zegura et al. 2011), while small doses over a long period of time can lead to tumor formation and metastasis (Ueno et al. 1996; Zhou et al. 2002).

One of the proposed methods of naturally regulating the composition and longevity of cHABs is the presence of viruses that infect cyanobacteria like *M. aeruginosa*, called cyanophages (Suttle 2000; Steenhauer et al. 2014; Xia et al. 2013). These phages are suspected to play a significant role in the control of cHABs but are still in the early stages of discovery. It is estimated that viruses are present in large numbers in aquatic environments, sometimes at concentrations of  $10^6$  particles per mL, and are

highly diverse, with a phage for every bacterial type (Pearl and Otten 2013). The most common toxic cyanobacteria in freshwater are *Microcystis* spp., *Cylindrospermopsis raciborskii*, *Planktothrix rubescens*, *Planktothrix agardhii*, *Synechococcus* spp., *Gloeotrichia* spp., *Anabaena* spp., *Lyngbya* spp., *Aphanizomenon* spp., *Nostoc* spp., some *Oscillatoria* spp., *Schizothrix* spp., and *Synechocystis* spp. (WHO, 2009). Of the currently isolated cyanophages, the majority have a host range that includes more than one of the genera listed above. For example, the LPP group is a group of phages that can infect *Lyngbya*, *Phormidium*, and *Plectonema*, which are all in the same order of cyanobacteria (Pandani and Shilo 1973), while the AS group can infect *Anacystis* and *Synechococcus*, and SM group can infect *Synechococcus* and *Microcystis* (Xia et al. 2013).

Only a handful of isolated cyanophages are specific for *M. aeruginosa*. Deng and Hayes (2008) isolated 35 wild type phages, of which 11 were only successfully propagated on *M. aeruginosa*, meaning they were species specific. The remaining wild phages could either infect a single other species of cyanobacteria or more than one species. They suggest that a few phages could infect across genera, for example both *Microcystis* and *Anabaena*, and noticed that when the phage could grow on multiple hosts, it had been isolated during a period of dominant species shift within the cHAB (Deng and Hayes 2008). Tucker and Pollard (2005) isolated a phage that was able to infect *M. aeruginosa*, called Ma-LBP. The phage was lytic in its host, and host lysis in the wild was positively correlated with the concentration of cyanophages in an Australian subtropical lake. Rodriguez-Valera et al. (2009) took a more general approach by studying the genomics of the composition of a cHAB. They note that many of the genes that differ between the strains and genera of cyanobacteria present in a cHAB are

potential phage recognition targets, which suggests that the diversity of prokaryotic populations is preserved by phage predation. Co-evolution between a phage and its host is further supported by Nakamura et al. (2014), who found genetic similarity in a 2.4 kbp segment of the phages DNA between Ma-LMM01-type phages isolated from the same lake and greater genetic differences in that same DNA sequence of Ma-LMM01-type phages from different locations, suggesting that phages rapidly diversify based on location and prevalence of their hosts.

The most extensively studied cyanophage for *M. aeruginosa* is Ma-LMM01, which is a 160 kbp DNA cyanophage that has been the primary focus of several studies that have come out of Dr. Takashi Yoshida's lab in Japan (Yoshida et al. 2006, 2008, 2014). This cyanophage has been shown to cause a lytic infection in *M. aeruginosa* strain NIES298 and has such a unique genome that was assigned a new lineage in the *Myoviridae* family (Yoshida et al. 2006). While the phage is lytic in NIES298, it is not readily lytic in other strains, so it is believed that Ma-LMM01 can infect only this one strain of *Microcystis* (Yoshida et al. 2006). Even within its host, the phage has some unique infection patterns. When the researchers infected the host with a multiplicity of infection (MOI, or ratio of virus particles to host cells),  $>1$ , there was only a small decrease in the number of host cells, and complete lysis of an entire culture was not obtained. With an MOI of 0.72–0.9, a decrease in the number of cells occurred within 12 hours post infection, and again, culture lysis was not complete. With an MOI  $<0.1$ , almost complete lysis of the host occurred, which included a clearing of the culture (Yoshida et al. 2006). Upon further study, it was discovered that within the host population, there were some cells that were resistant to infection. A sub-culture of

NIES298 was established and infected, and the host cell numbers increased post infection but the growth rate was lower than non-infected controls. The sub-strain showed intermediate sensitivity, suggesting co-existence of both sensitive and resistant cells in culture. Yoshida et al. (2014) proposed that this relationship might be due to a growth rate cost for viral resistance, but could not determine if there was a difference in adsorption between the phage-sensitive and phage-resistant sub strains. During the infection process, Ma-LMM01 does not induce down regulation of *M. aeruginosa* housekeeping genes, which may indicate that the virus requires the maintenance of host transcription and that severe modification of the host genome would induce the hosts CRISPR (clustered regular interspaced short palindromic repeats)-Cas (CRISPR-associated genes) defense system (Honda et al. 2014).

A notable gene of the Ma-LMM01 genome includes a homologue of the *nblA* (*nonbleaching*) genes found in cyanobacteria and red algae (Yoshida et al. 2008; Yoshida-Takashima et al. 2012). In cyanobacteria, *nblA* degrades the phycobilisomes (PBS), or major light-harvesting complexes of the photosynthetic apparatus. During nitrogen starvation, cyanobacteria degrade the PBS to cause “bleaching,” which is a defense mechanism to prevent photodamage caused by the absorption of excess light energy and to provide the energy needed for cellular acclimation (Baier et al. 2004). The degradation of the PBS and the decline of host photosynthesis may be more beneficial to the phage than sustaining photosynthesis, as saltwater phages do, as the degradation may be required to decrease photodamage as the phage replicates. It may also be that degradation of the PBS provides amino acids for phage protein synthesis (Yoshida et al. 2008).

While current studies indicated that Ma-LMM01 is strictly lytic, the cyanophage also has a number of genes not typically found in lytic phages, such as a site-specific recombinase homologue and a flanking transposase gene homologue, which are frequently used by temperate phages to integrate the phage genome into the bacterial chromosome (Groth and Calos 2004). This might mean that the phage could be lysogenic in potential hosts or that the phage acquired the genes through transposable element transfer. Finally, there is an ORF in the Ma-LMM01 genome that shows significant sequence similarity to the *E. coli phoH*, which is an ATPase that is induced under phosphate starvation. This is common among marine cyanomyoviruses (Chen and Lu 2002; Man et al. 2005; Sullivan et al. 2005), but the habitat of Ma-LMM01 and NIES298 is a eutrophic phosphate rich lake in Japan, so it is unclear why the phage would have this gene.

There is a lack of information on how viruses affect the growth of cyanobacterial hosts *in situ*. Because Ma-LMM01 is a lytic phage in its host strain NIES298, we can use this system to model lytic viruses during the formation of a bloom. In particular, we are interested in discovering how modified nutrient availability will change the growth conditions for the host and the replication of the phage. The increase in the prevalence of cHABs is related to the nutrient over-enrichment of freshwater and marine ecosystems from urban, agricultural, and industrial sources (Paerl and Paul 2011; Paerl et al. 2011). Phosphorus excess from these sources has contributed to the increased prevalence of cHABs in freshwater ecosystems, but nitrogen-rich aquatic ecosystems (high N:P) can also be plagued by cHABs, especially non-N<sub>2</sub>-fixing genera like *Microcystis* and *Plankthothrix* (Paerl and Fulton 2006). Nutrient-enriched water bodies are especially

prone to cHABs if they have long residence times, water temperatures periodically exceeding 20°C, calm surface waters, and persistent vertical stratification (Paerl and Otten 2013). Previous studies examining relationships between nutrient availability and cHABs have discovered that non-toxin-producing strains require lower nutrient concentrations to reach maximum growth than toxin producing strains (Rapala et al. 1997), but toxin-producing strains can outgrow non-toxin-producing strains at high levels of nitrogen concentrations (Vezie et al. 2002). One effect of phosphorus on the growth of *M. aeruginosa* and the production of MCs is that small changes in phosphorus concentrations have a significant effect on cellular growth (Vezie et al. 2002), but extreme changes in the concentration at either end will have an increased effect on the production of MCs (Sivonen et al. 1990; Oh et al. 2000; Vezie et al. 2002).

In 2008, M. Yoshida and colleagues studied how cyanophages effect the dynamics of a cHAB in the wild and found that there were seasonal dynamics to the bloom which related to the shift in toxin- and non-toxin-producing strains of *M. aeruginosa*. Early in the season (May–June), there was an increased presence of the viruses and a decreased presence of the hosts, but no significant correlation was found between the increase in viral presence and environmental conditions such as nutrient composition of the lake. Understanding that nutrient loading can have a relationship to the species composition of cHABs. The following research analyzes the relationship between Ma-LMM01 and its host, NIES298, under some modified nutrient conditions in a lab controlled setting. The hypothesis of this study is that because *Microcystis* growth is greatly affected by changes in nitrogen and phosphorus concentrations, we should see a change in viral replication as the nutrient concentrations change. Specifically, we focus

on the relationship between phosphorus limitation and viral infection, knowing that the phage has a homologue *phoH* gene, which may allow the phage to modify expression of host *phoH* genes to enhance phage propagation under phosphorus-limited host stress. We test the idea that a viral infection by Ma-LMM01 will magnify the negative effect phosphorus limitation has on the growth rate and carrying capacity of a *M. aeruginosa* NIES298 population.

## Materials and Methods

### 2.1 Cell Culture and Maintenance

Strains of *Microcystis aeruginosa* were obtained from the National Institute of Environmental Studies Japan Culture Collection (NIES), which were all unialgal, and from the Great Lakes Environmental Research Laboratory (GLERL), which were predominately mixed cultures (Table 1). The cell cultures were grown for experimentation at 30°C using a 12:12 hour light:dark cycle of 40  $\mu\text{mol photons m}^{-2}\text{s}^{-1}$  under cool white fluorescent illumination in a Conviron ATC10 standing growth chamber (Manitoba, Canada) as previously described (Yoshida et al. 2006; Yoshida et al. 2008). The cells were maintained in CB Media. CB medium has the following composition (in milligrams per liter of deionized distilled water):  $\text{Ca}(\text{NO}_3)_2 \cdot 4\text{H}_2\text{O}$ , 150;  $\text{KNO}_3$ , 100;  $\text{MgSO}_4 \cdot 7\text{H}_2\text{O}$ , 40;  $\beta$ -disodium glycerophosphate, 50; bicine, 500; biotin, 0.0001; vitamin B12, 0.0001; and thiamine hydrochloride, 0.01, with 3 ml of PIV metals. PIV metals consisted of the following (in milligrams per 100 ml of deionized distilled water):  $\text{FeCl}_3 \cdot 6\text{H}_2\text{O}$ , 19.6;  $\text{MnCl}_2 \cdot 4\text{H}_2\text{O}$ , 3.6;  $\text{ZnCl}_2$ , 1.04;  $\text{CoCl}_2 \cdot 6\text{H}_2\text{O}$ , 0.4;  $\text{Na}_2\text{MoO}_4 \cdot 2\text{H}_2\text{O}$ , 0.25; and disodium EDTA  $\cdot 2\text{H}_2\text{O}$ , 100. The pH of CB media was adjusted to 9.0 (Kasai et al. 2004). CB media was sterilized in an autoclave at 121°C for 15 minutes (Shirai et al. 1989).

When not being grown for experimentation, the *M. aeruginosa* cultures were maintained in CB media under sub-optimal conditions at 25°C under ambient light near a window on a laboratory bench top for approximately a 10:14 hour light:dark cycle. Strains were serially transferred every month at a 1:100 dilution. Cultures were visually monitored for changes in color and sedimentation every week, and when needed, visually



assessed with a microscope (Culture recommendations; NIES Culture Collection, Japan 2001). Additionally, samples of each culture were cryopreserved in liquid nitrogen in 4% DMSO per Watanabe and Sawaguchi (1995). Storage in methanol is also possible, but storage in glycerol is not recommended.

The Ma-LMM01 viral stock used in this study was provided by the Yoshida lab as a phage water sample in 2 mL aliquots. The majority of the phage samples were stored at -80°C, with some samples at 4°C, and one sample stored at room temperature. The titer of the -80°C stored stocks were estimated based on genomic copy numbers as  $5.6 \times 10^4$  -  $5.6 \times 10^5$  genomes per mL, as determined using a serial dilution qPCR series.

Table 1. *Microcystis aeruginosa* strains and the cyanophage used in this study, including the location of origin and toxin producing ability.

Strain of <i>M. aeruginosa</i>	Toxic potential	Isolation location	Obtained from	Culture State
NIES298	Toxin producer	Lake Kasumigaura, Japan	NIES Culture Collection	Unialgal
NIES90	Toxin producer	Lake Kawaguchi, Japan	NIES Culture Collection	Unialgal
NIES44	Non-toxic	Lake Kasumigaura, Japan	NIES Culture Collection	Unialgal
CPCC124	Non-toxic	Heart Lake, Ontario	Dr. Tim Davis, NOAA (GLERL)	Unialgal
LE3	Toxin producer	Lake Erie, USA	Dr. Tim Davis, NOAA (GLERL)	Mixed
LB2386	Non-toxic	Little Rideau Lake, Ontario	Dr. Tim Davis, NOAA (GLERL)	Mixed
LB2385	Toxin producer	Little Rideau Lake, Ontario	Dr. Tim Davis, NOAA (GLERL)	Mixed
Ma-LMM01 (virus)	-	Lake Mikata, Japan	Dr. Takashi Yoshida	-

## 2.2 Growth Quantitation of *Microcystis aeruginosa*

Growth of *M. aeruginosa* was monitored for a period of 10–14 days by measuring optical density at 600 nm in a UV/Vis Spectrophotometer 1000 (Ward's Science, Rochester, NY). Absorbance readings were validated in triplicate with direct cell counts using a hemocytometer (Neubauer, 0.1 mm depth) in duplicate at 400x magnification (Guillard 1978; Tas et al. 2006). While adapted laboratory strains no longer exhibit colonial morphology, *M. aeruginosa* still frequently forms dyad complexes, which were subjected to high-speed vortexing for 30–60 seconds to separate them (Humphries and Wijaja 1979).

## 2.3 DNA Extraction and Quantitative Polymerase Chain Reaction (qPCR)

For both *M. aeruginosa* and Ma-LMM01 genome extractions, DNA was isolated using the potassium xanthogenate-sodium dodecyl sulfate (XS-SDS) protocol (Tillett and Neilan 2000). For restriction digest DNA samples, 1 mL of mid to late logarithmic growth phase cultures were harvested by centrifugation (12,000 x g for 10 minutes) and resuspended in 50 µL TE Buffer (10 mM Tris-HCL, 1 mM EDTA). For all other experimental samples, 250 µL of cell suspension was extracted. To each cell suspension, 750 µL of freshly made XS Buffer (1% potassium ethyl xanthogenate; 100 mM Tris-HCL, 20 mM EDTA, 1% sodium dodecylsulfate, 100 mM ammonium acetate) was added and inverted to mix. The samples were incubated at 70°C for 30 minutes with vortexing every 10 minutes.

After the incubation period, the samples were placed on ice for another 30 minutes, after which the cellular debris was collected by centrifugation at 12,000 x g for 10 minutes. The supernatant fluid was removed to a clean tube with 750 µL isopropanol

and allowed to sit at room temperature for a minimum of 10 minutes, or stored at -20°C overnight. The sample-isopropanol mixture was then centrifuged to pellet the precipitated DNA at 12,000 x g for 10 minutes, and the supernatant fluid was decanted. The DNA pellet was washed with 70% ethanol and air dried before being re-suspended in 200 µL of TE Buffer. DNA samples were stored at -80°C.

Amplification of cyanobacteria and cyanophage genes was achieved using qPCR. Each 20 µL reaction contained 10 µL 2x qPCR SyGreen Blue Mix Lo-ROX (PCR BioSystems), 0.8 µL 10 mM Forward Primer, 0.8 µL 10 mM Reverse Primer, either 5 µL sample or 100 ng DNA, and ddH<sub>2</sub>O. The qPCR was run on a BioRad Chromo 4 real-time PCR detector (BioRad, California, USA) and consisted of an initial denaturing step for 30 seconds at 90°C, followed by 35 cycles of 95°C for 5 seconds, 58°C for 30 seconds, and 78°C for 30 seconds. A melting curve analysis was performed from 65°C–95°C. The primers used in the following experiments are listed in Table 2. Where applicable, cycle threshold (Ct) values for cyanophage genes were calculated against *gyrB* (bacterial gyrase B) transcripts as an internal control gene using the  $2^{-\Delta\Delta C_t}$  equation (Livak and Schmittgen 2001), where  $\Delta\Delta C_t = (C_{t_{gyl}} - C_{t_{gyrB}})_{Time\ x} - (C_{t_{gyl}} - C_{t_{gyrB}})_{Time\ 0}$ , where Time x is a specific time point during the infection (Figure 1).

Table 2. List of DNA primers for qPCR used in this study.

Organism	Gene	Sequence (5'-3')	Function	Obtained from
Ma-LMM01	<i>nblA</i>	F GTGAGTGCCATTCTGC	Early viral gene, responsible for a phycobilisome degradation protein	Yoshida et al. 2006
		R TCTTCTTGATGATAGCCGC		
	<i>g91</i>	F ACATCAGCGTTCGTTTCGG	Late viral gene, is a phage structural protein (tail sheath)	Honda et al. 2014
		R CAATCTGGTTAGGTAGGTCG		
<i>Microcystis aeruginosa</i>	<i>gyrB</i>	F TTACACGGAGTCGGGATTTC	DNA repair and recombination protein	Honda et al. 2014
		R AAACGTCCGGAGAGGGTACT		
	<i>sigA</i>	F CGCCGATCAATCCCGCACCA	Transcription Principal sigma factor	Honda et al. 2014
		R CTCGGTGGGTTTGCACGCA		
	<i>gyrB</i> 53F-354R	F GTCGCCTATATGTGTCGGGAA	DNA repair and recombination protein	This study <sup>1</sup>
		R TTCCGGTTCGGGGACTTTTA		
	<i>mcyB</i>	F CCTACCGAGCGCTTGGG	Microcystin gene B (toxin)	Kurmayer and Kutzenberger 2003
		R GAAAATCCCCTAAAGAATCCT GATTCCTGAGT		

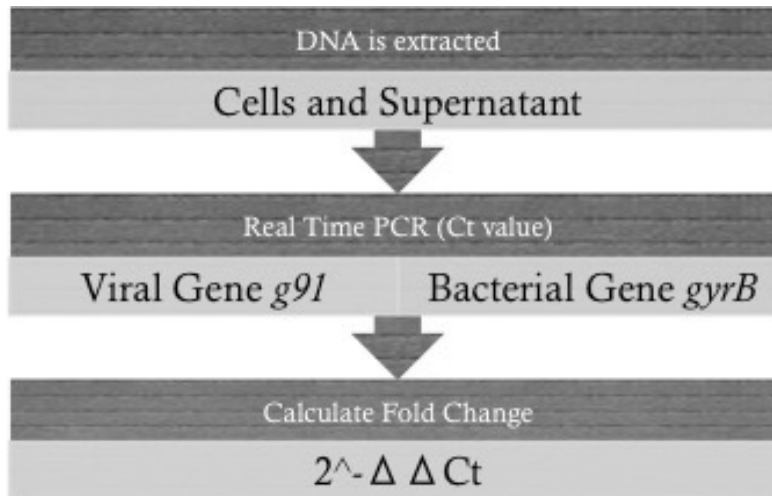


Figure 1. Flow chart of the relative viral genome replication methodology used in this study.

<sup>1</sup> GenBank: AB325146.1

## 2.4 Strain Identification using Restriction Digest Profiles

Three genes, *sigA*, *gyrB*, and *gyrB53F-354R*, were amplified using PCR for each strain of *Microcystis aeruginosa* listed in Table 1 and tested against a series of restriction enzymes to establish a unique strain profile. The potential enzymes were chosen by checking the published sequences for these three genomic loci within the whole genomic sequence of *M. aeruginosa* NIES843 (GenBank: AP009552.1) for complete or single nucleotide deviations from the enzyme recognition sequence. The chosen enzyme and gene combinations tested are listed in Table 3.

Restriction digest of the amplified products were performed in 50 µl reactions, which consisted of 1 µg of DNA, 5 µl of 10x CutSmart Buffer (NEB, Ipswich, MA), 1 µL (10 Units) of restriction enzyme<sup>2</sup> (Table 3), and ddH<sub>2</sub>O. The reactions were incubated in a water bath set for 37°C for 1 hour. Samples were then analyzed on a 2% agarose gel for differences in banding pattern, and any remaining digested samples were stored at -20°C.

Table 3. Potential restriction enzyme and gene combinations to create a restriction digest profile.

Enzyme	<i>sigA</i>	<i>gyrB</i>	<i>gyrB53F-354R</i>	Sequence (5'-3')
<i>Bam</i> HI	X			GGATCC
<i>Pst</i> I		X	X	CTGCAG
<i>Eco</i> RV			X	GATATC
<i>Age</i> I (PinAI)			X	ACCGGT
<i>Msp</i> I ( <i>Hpa</i> II)	X	X	X	CCGG
<i>Eco</i> RI		X	X	GAATTC
<i>Hinf</i> I	X	X		GANTC
<i>Sal</i> I		X		GTCGAC

<sup>2</sup> Enzymes obtained from NEB, Ipswich, MA

## 2.5 Viral Infection

Ma-LMM01 was obtained from the Yoshida lab and was stored at  $-80^{\circ}\text{C}$  in 2 mL aliquots, per the conditions published by Yoshida et al. (2006). Late logarithmic growing cultures of *M. aeruginosa* were diluted into either 5 mL or 25 mL fresh media to an optical density of 0.08–0.12 (approximately  $5 \times 10^5$ – $7.5 \times 10^5$  cells/mL), and infected at a MOI of  $10^{-1}$ – $10^{-2}$ . All infections occurred in standard CB media, unless otherwise noted. The infections were placed in standing growth chambers under the conditions mentioned in section 2.1. Samples were monitored for differences in optical density, and periodically throughout the infection growth period, 0.5 mL samples were removed and stored at  $-80^{\circ}\text{C}$  for later DNA extraction and analysis of viral genes. During the modified media tests, CB media was modified based on the phosphorus and nitrogen concentrations studied in Vezie et al. (2002), which modified a different cyanobacteria growth medium (Table 4). Samples were analyzed for a difference in growth curves in comparison to viral genome replication, per the method outlined in Figure 1.

### 2.5.1 Characterization of Viral Infection

A sample of each late logarithmic growing cultures from *M. aeruginosa* NIES298, LE3, CPCC124, LB2385, and LB2386 were tested for a viral infection where complete clearing of the cultures due to complete host lysis did not occur. The host cultures were diluted and infected with the viral stock stored at  $-80^{\circ}\text{C}$ . Negative controls consisted of uninfected cultures that were diluted to the same approximate cellular density, as determined by absorbance readings, and cultures infected with room temperature stored virus (which were inactivated due to improper storage for a prolonged

period of time). The replicate tubes were monitored approximately every day for 13 days for changes in optical density and compared to the changes published by Yoshida et al. (2014). Samples were analyzed for a difference in growth curves in comparison to viral genome replication.

### **2.5.2 Limited Phosphorus and Nitrogen Infection, Trial 1**

A large single batch culture of *M. aeruginosa* NIES298 was infected with Ma-LMM01 and incubated for 20–24 hours in standard CB media to promote viral attachment, absorption, and initiation of viral replication. Both infected and uninfected samples were harvested at 11,750 x g for 15 minutes at 6°C. The supernatant fluid was removed (which includes any unattached virus) and the cells resuspended and standardized to an absorbance reading of 0.12 at 600 nm (approximately  $7.5 \times 10^5$  cells/mL) prior to splitting into replicates in either CB control or nutrient modified media (Figure 2): Mid P, Low P, Low N (Table 4). Four replicate samples per nutrient treatment were placed in borosilicate glass test tubes and were not vortexed prior to optical density readings and removal of a sample for DNA extraction, which may have led to a sample bias based on the location in the water column from which the sample OD was being read and from where the sample for DNA extraction was being removed. Each culture sample that was removed for DNA analysis was extracted twice and analyzed for a difference in growth curves in comparison to viral genome replication, as described in section 2.6.

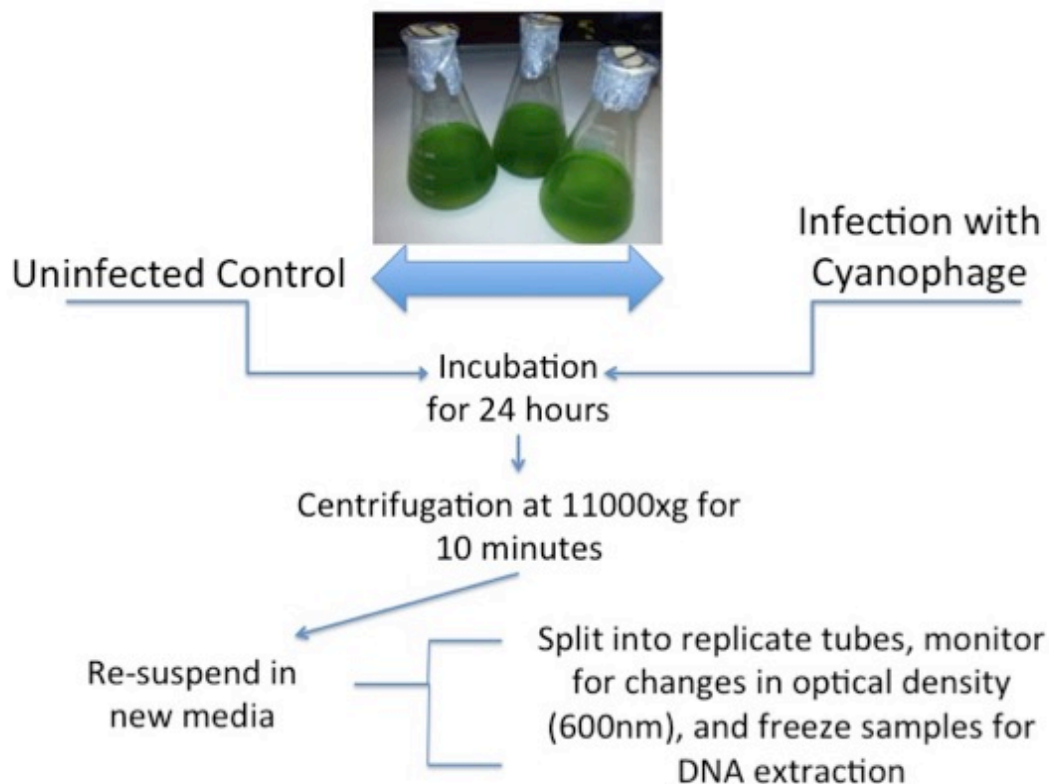


Figure 2. General outline of the methodology used in the nutrient-modified infection trials.

### 2.5.3 Limited Phosphorus and Nitrogen Infection, Trial 2

A large single batch cultures of *M. aeruginosa* NIES298 was diluted into either new control media or nutrient modified media and equalized to an absorbance reading of 0.12 at 600 nm (approximately  $7.5 \times 10^5$  cells/mL) prior to infection (Table 4). Each replicate tube was inoculated with the phage; therefore, viral infection occurred in the nutrient-limited media, and no removal of the viral supernatant occurred. The four replicate nutrient samples were then treated as described in trial 1 (section 2.5.2), the samples were placed in borosilicate glass test tubes and were not vortexed prior to optical density readings and removal of a sample for DNA extraction, which may have led to a sample bias based on the location in the water column from which the sample OD was



being read and from where the sample for DNA extraction was being removed. Each culture sample that was removed for DNA analysis was extracted twice and analyzed for a difference in growth curves in comparison to viral genome replication, as described in section 2.6.

#### 2.5.4 Phosphorus Limited Trial

A large batch culture of *M. aeruginosa* NIES298 was infected with Ma-LMM01 at a lower MOI compared to the previous trials, at  $10^{-3}$ – $10^{-4}$ , and incubated for 20–24 hours to promote viral attachment. Both infected and uninfected samples were harvested at 11750 x g for 10 minutes at 6°C. The supernatant fluid was removed and the cells resuspended in either control or nutrient modified media (Table 4), similar to the method in trial 1. The phosphate limited and control samples (25 mL) were grown in glass Erlenmeyer flasks, and swirled prior to sample analysis and removal. Each culture sample that was removed for DNA analysis was extracted once (due to the large number of replicate samples extracted) and analyzed for a difference in growth curves in comparison to viral genome replication, as described in section 2.6.

Table 4. Modifications of CB media to assess the impact of nutrient conditions on phage infection

Media	P *(mg/L)	N <sup>+</sup> (mg/L)	Na # (mg/L)	N:P Ratio	Trial Used
<b>CB Control</b>	7.17	31.64	-	9.76	1, 2, 3
<b>CB Mid P</b>	0.11	31.64	-	636.29	1, 2
<b>CB Low P</b>	0.05	31.64	-	1339.84	1, 2, 3
<b>CB Low P with ion compensation</b>	0.05	31.64	19.24	1399.84	3
<b>CB Low N</b>	7.17	8.4	-	2.59	1, 2

\*For phosphorus modifications, the concentration of  $\beta$ -disodium glycerophosphate was changed. +For nitrogen modifications, the concentrations of both  $\text{Ca}(\text{NO}_3)_2 \cdot 4\text{H}_2\text{O}$  and  $\text{KNO}_3$  were changed. #For ion compensations, the  $\beta$ -disodium glycerophosphate concentration was changed, and the difference was supplemented with NaCl.

## 2.6 Statistical Analysis

Growth rates and maximum optical density at stationary phase were determined using non-linear regression analysis using the formula:

$$(\text{SAMPLE} \sim K * 0.12 * \exp(R * x) / (K + 0.12 * (\exp(R * x) - 1)))$$
, where the SAMPLE is the optical density at each time point collected (x), K is the carrying capacity of the population (stationary phase), and R is the population specific growth rate. To determine if there were statistical differences in the growth rate between infected and uninfected samples within specific trials, two-way analysis of variance (ANOVA) was applied to each nutrient-modified set of replicates. When ANOVA was significant, Tukey's post hoc comparisons were performed. For within group comparisons, a paired T-test was used. R statistical software version 3.3.2 was used for all statistical analyses.

## Results

### 3.1 Growth Quantitation of *Microcystis aeruginosa*

Newly seeded *Microcystis aeruginosa* NIES298 cultures grown under standard conditions (section 2.1) were monitored for changes in optical density using absorbance readings at 600 nm. A single trial of five identically seeded cultures was quantitated by spectrophotometry (Figure 3). From each culture, 2 aliquots were removed for manual cell counts at each time point using a hemocytometer. The averages of these counts were plotted (Figure 4), and the logistic relationship was used to estimate the number of cells in solution in later trials.

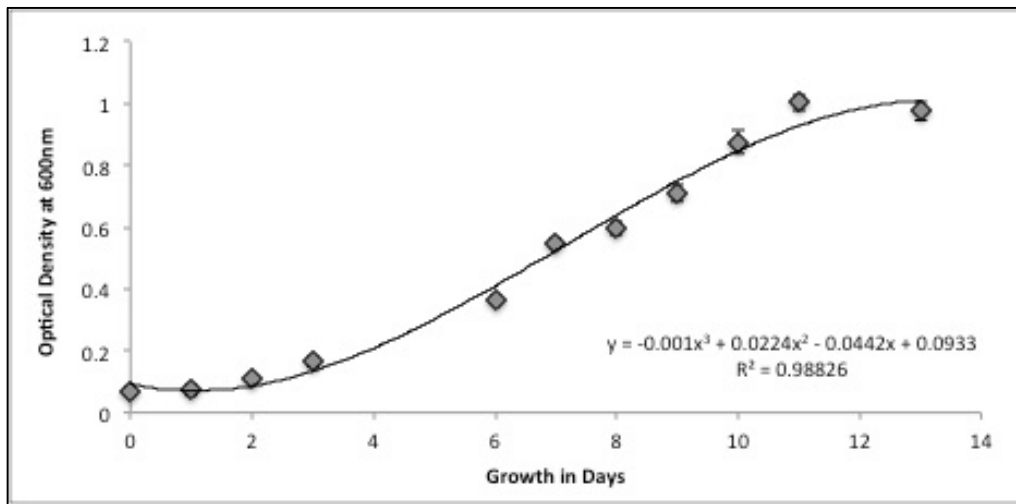


Figure 3. Growth curve of *M. aeruginosa* using UV/Vis spectrophotometry. This relationship was fitted with a logistic curve, with an  $R^2$  value of 0.988.

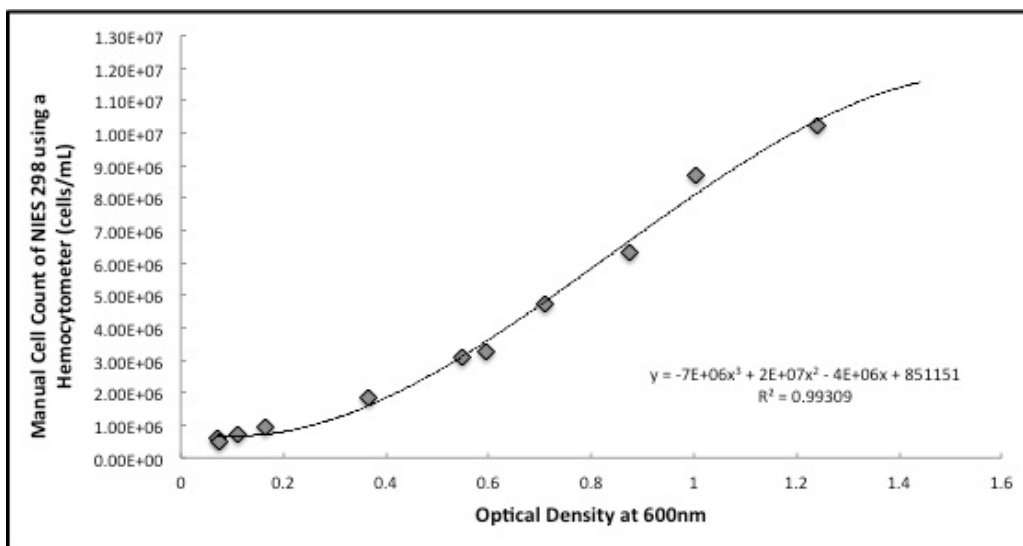


Figure 4. Growth of *Microcystis aeruginosa* NIES298 using UV/Vis spectrophotometry and manual cell counts. Manual cell counts were averaged and plotted against the average absorbance reading of replicate control tubes. The relationship was fitted with a logistic line, with an  $R^2$  value of 0.99.

### 3.2 Strain Identification using Restriction Digest Profiles

The *Microcystis aeruginosa* strains used in this study are all laboratory accustomed, which means that they no longer display colonial morphology. Additionally, these strains are all morphologically identical, and not every strain is unialgal. In order to establish the identity of each strain and to identify any potential future strain cross-contamination, a restriction digest profile was created for the strains used in this study. The 7 strain isolates of *M. aeruginosa* (Table 1) were cultured to late logarithmic growth phase in standard CB Media prior to collection for DNA extraction. Three *M. aeruginosa* genetic loci (*gyrB*, *sigA*, and *gyrB53F-354R*) were chosen for amplification using PCR, and the sequences were tested for restriction digest sites (Table 3). The enzyme-gene combinations were visualized on a 2% agarose gel, and the successful enzyme-gene combinations were repeated (Figure 5A). The *MspI* restriction enzyme cuts *gyrB* in NIES298, NIES90, and LE3. *MspI* was also used with *sigA*, which had a recognition site

in NIES90, CPCC124, LB2386, and LB2385. A double digest was preformed on *gyrB53F-354R* using *XbaI* and *HpaI*, which does not cut NIES90, cuts NIES44 twice, and the others once. As an additional measure of identification, the toxin potential of each strain was tested by PCR amplification of a microcystin gene B (*mycB*) (Figure 5B). A positive band of ~100 bp was generated using DNA from NIES298, NIES90, LE3, and LB2385, which is consistent with published strain toxin ability. Faint banding patterns and larger amplified products were generated in NIES44, CPCC124, and LB2386, which are published non-toxin-producing strains, so the bands are not likely due to the presence of *myc* genes.

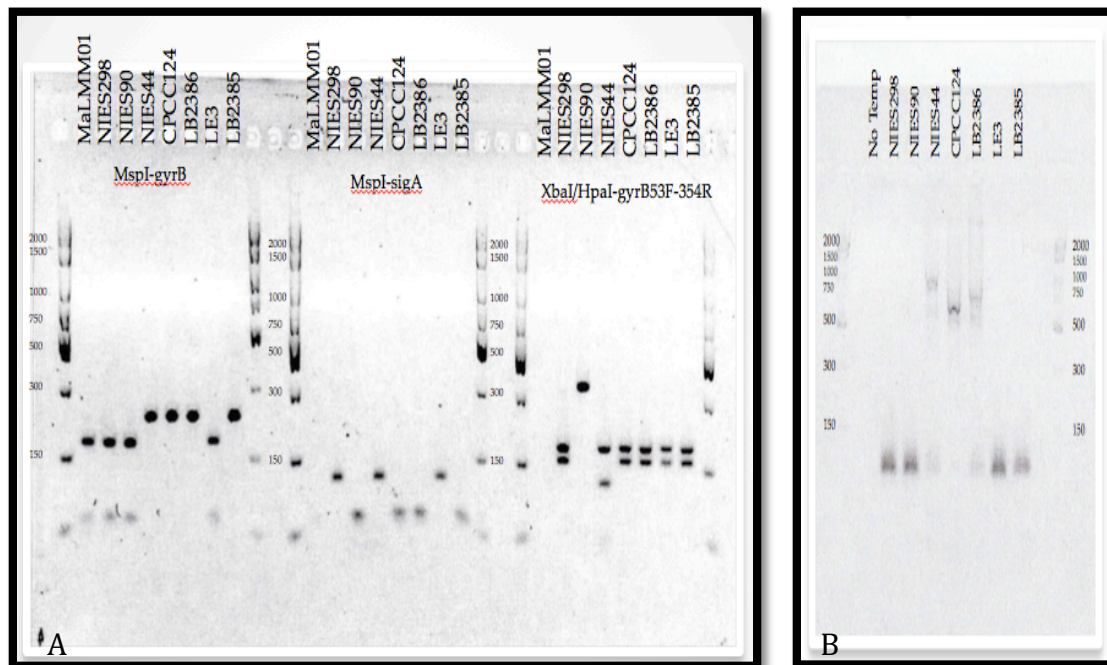


Figure 5. Strain identification based on restriction digests of the amplified cyanobacterial genes analyzed on 2% agarose gel. **A.** Restriction digest profile of the strain isolates used in this experiment. Restriction enzyme *MspI* was used on *gyrB* and *sigA*, and a double digest using *XbaI* and *HpaI* was used on *gyrB53F-354R*. Uncut *gyrB* gives a band about 250 bp, uncut *sigA* gives a band of about 125 bp, and uncut *gyrB53F-354R* gives a band of about 425 bp. **B.** Visualization of the presence or absence of *MycB* gene for each strain. A positive band for *MycB* gene is 78 bp.

The restriction enzyme profile and the presence or absence of a *mycB* band data were combined with a visual confirmation of the strain purity using a microscope to verify the identity of strains through the presence or absence of other algal species (Table 5). Without the visual confirmation that the culture is unialgal, the profiles of NIES298 and LE3 are the same, and the profiles of CPCC124 and LB2386 are the same.

Table 5. Summary of molecular profiles of the strains of *Microcystis aeruginosa* used in this project

Enzyme-Gene	NIES298	NIES90	NIES44	CPCC124	LB2386	LE3	LB2385
MspI- <i>gyrB</i>	2	2	1	1	1	2	1
MspI- <i>sigA</i>	1	2	1	2	2	1	2
XbaI & HpaI- <i>gyrB53F-354R</i>	2	1	3	2	2	2	2
<i>McyB</i>	+	+	-	-	-	+	+
Strain Purity	Unialgal	Unialgal	Unialgal	Unialgal	Mixed	Mixed	Mixed

### 3.3 Presence of Viral Genes in *M. aeruginosa* Genomes, Pre-Infection

Prior to the introduction of the phage to any of the strains of *M. aeruginosa*, the DNA from 1 mL of late logarithmic growing cultures of all strains of *M. aeruginosa* (Table 1) and 250 µL of Ma-LMM01 phage sample were extracted. The presence and relative increase of viral sequences in these samples was determined by qPCR amplification of viral *g9I* and *nblA* primer sets (Table 2). The PCR products were run on a 2% agarose gel and imaged on BioRad Molecular Imager ChemiDoc XRS+ Imaging System (BioRad, Hercules, California) (Figure 6). When using the *g9I* primers, LE3 consistently gave a band of about 500 bp, which is also seen in LB2386 and occasionally in LB2385 (not shown). A secondary band can be seen in LE3 at about 700 bp, and a faint band at about 850 bp is in CPCC124. Upon repetition, no bands appeared for NIES298, NIES90, and NIES44. The Ma-LMM01 control band for *g9I* was at 140 bp.

Presence of viral *nblA* genes in the strains of *M. aeruginosa* CPCC124, LB2385, LB2386, and LE3 show a band around 250 bp, and a series of other bands higher than 500 bp, which can also be seen in NIES298 and NIES90. The Ma-LMM01 control band for viral *nblA* is at 200 bp. The presence of these bands is most likely due to cellular homologs, since *nblA* was originally a host gene (261 bp<sup>3</sup>), and can be found in a majority of cyanobacterial species.

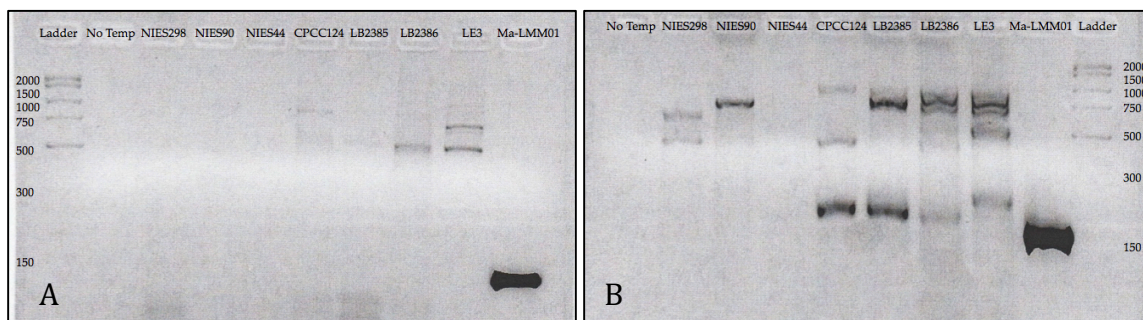


Figure 6. Initial analysis of phage genes g91 and *nblA* prior to infection, analyzed on a 2% agarose gel. **A.** Presence of g91 genes in the strains of *M. aeruginosa*. The Ma-LMM01 control band for g91 is at 140 bp. While there are some bands in the cyanobacteria, none are close to the size of the control band. **B.** Presence of viral *nblA* genes in the strains of *M. aeruginosa*. The Ma-LMM01 control band for *nbaA* is at 200 bp. There are bands that are close in size in CPCC124, LB2385, and LB2386, which may be host *nblA* genes (261 bp).

### 3.4 Characterization of Viral Infection

*Microcystis aeruginosa* NIES298 was cultivated and infection by Ma-LMM01 was characterized using molecular techniques. We infected the host with either a room temperature stored phage or a phage stored at -80°C and monitored the growth rate of five replicate cultures for 13 days (Figure 7A). Both the uninfected control samples and the room temperature stored phage infected samples had a higher growth rate than the -80°C stored phage infected samples, which was statistically significant ( $p < .05$ ) (Figure

<sup>3</sup> Genebank: NC\_010296.1

7B). In addition to a difference in the whole population growth rate, we monitored viral replication by using qPCR to quantitate the relative increase in genome copies of viral gene *g9I*. In the -80°C stored phage infected samples, the viral gene increased 100-fold by day 6 and maintained that level for the whole trial (Figure 7A). In the room temperature stored phage-infected samples, we get a 1000-fold decrease in the viral genomes relative to cellular genomes by day 13. A decrease in the viral gene *g9I* indicated that there was no viral replication occurring with the room temperature stored phage, while an increase in the viral gene *g9I* indicated that a combination of viral genome replication and host cell death was occurring with the -80°C stored phage. Infection with 4°C stored phage was comparable to the -80°C stored phage (data not shown).

With this trial, we also wanted to see if we could determine if there was cell-free virus as an indication of a productive infection. To do this, we compared the number of viral genomic copies found in infected cultures (which included both the host cells and the supernatant fluid) to those isolated from pelleted and washed cells from the same culture to determine if the source of the *g9I* signal was due to cell-associated genomes, extracellular genomes, or both (Figure 7C). The supernatant fluid was not tested on its own for this trial. Again using the presence of the viral gene *g9I* as an indicator for viral infection, we see that by day 6, we had a 100-fold increase in viral genomes, which was maintained until day 13. In the pelleted and triple-washed (with DI water) cell samples, we initially saw a higher ratio of viral genes to bacterial genes by day 2, which may correspond to viral attachment to the host cell. By day 6, we had approximately 100-fold increase in viral genomes, which is associated with the cell. In a successful lytic



infection, we would expect to see the viral genes associate with the host in a small time-frame, then increase in number before lysing the cell and disassociating from the host cells. What we observed was that the viral genomes increased, but did not disassociate from the host, and instead remained cell-associated post genome replication (Figure 7C).

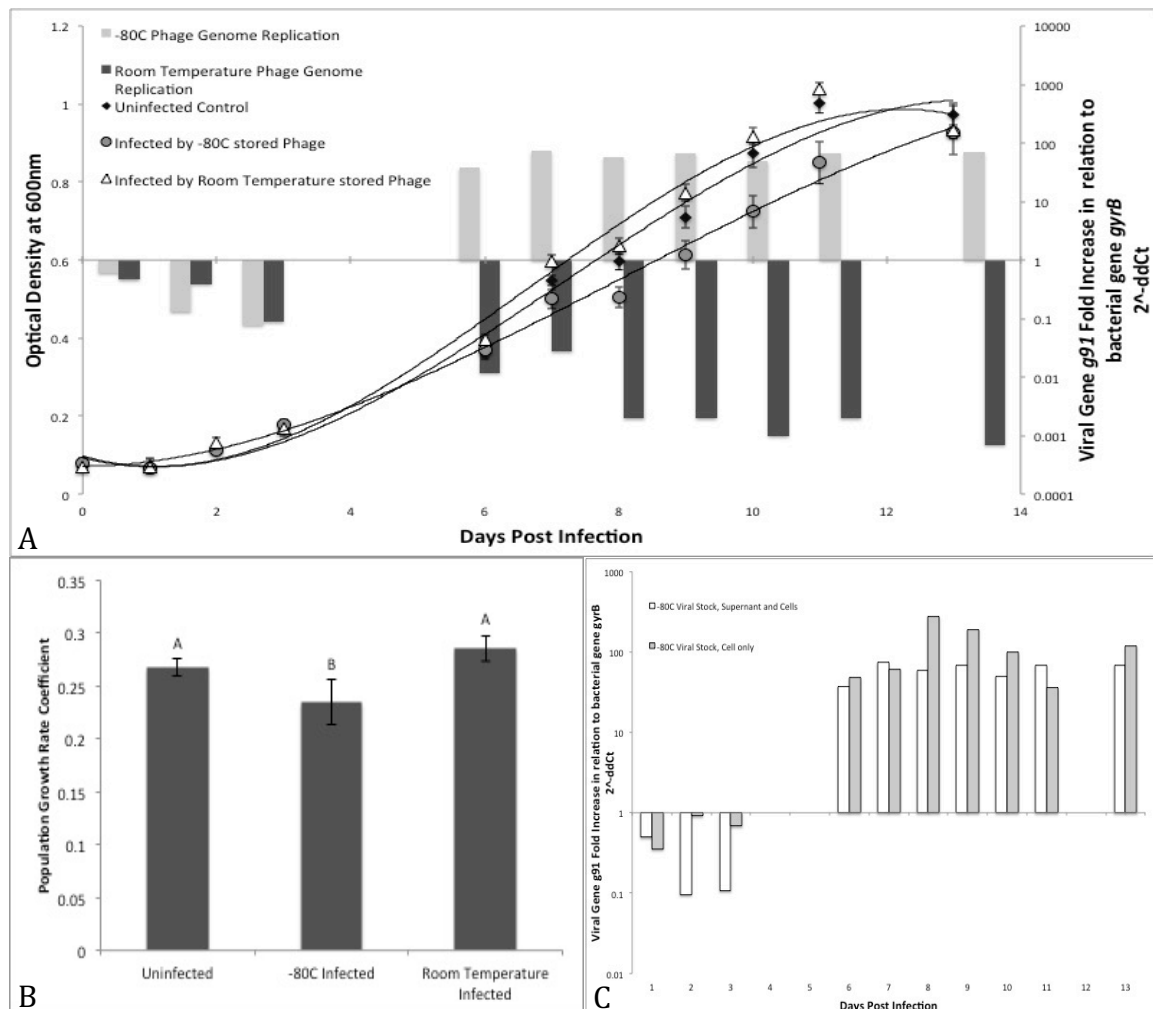


Figure 7. Verification of an infection in *M. aeruginosa* NIES298. **A.** Growth curves of uninfected samples, infected samples with an phage stored at  $-80^{\circ}\text{C}$ , and infected samples with an phage stored at room temperature. Relative viral genome replication in quantified using the Double Delta Ct equation ( $2^{-\Delta\Delta Ct}$ ), where a positive value indicates an increase in viral genomes as a proxy for a successful viral infection and a negative value indicates an unsuccessful viral infection. **B.** The growth rates between the infection with the phage stored at  $-80^{\circ}\text{C}$  ( $0.234 \pm 0.022$ ) and the infection with the phage stored at room temperature ( $0.285 \pm 0.011$ ) were statistically different ( $p < .05$ ). The uninfected growth rate is  $0.268 \pm 0.009$ . Error bars represent standard deviation of five replicate culture tubes. **C.** Estimation of viral location during infection. There was not a large difference between the genomes recorded between whole infected culture samples and the cell only samples.

### 3.5 Host Specificity Test

To verify the specificity of the host range of Ma-LMM01 and to ensure that an increase in genomes was related to the difference in growth rates between the uninfected and infected samples, three other strains of *M. aeruginosa* were tested: CPCC124, LB2385, and LB2386 (Table 1). The growth of six replicates of each culture was monitored using optical density for 13 days post infection, and the DNA was extracted for analysis of viral genome replication (Figure 8). *M. aeruginosa* NIES298 saw an increase in viral genomes by day 6, similar to the growth seen in the verification of infection trial, and a difference in growth rates between the infected and uninfected samples ( $p < .01$ ) (Figure 8A, 8E). In the other tested strains of *M. aeruginosa*, there was no positive replication of the phage (Figure 8B, 8C, 8D), and no significant difference in the growth rates between the infected and uninfected samples (Figure 8E).

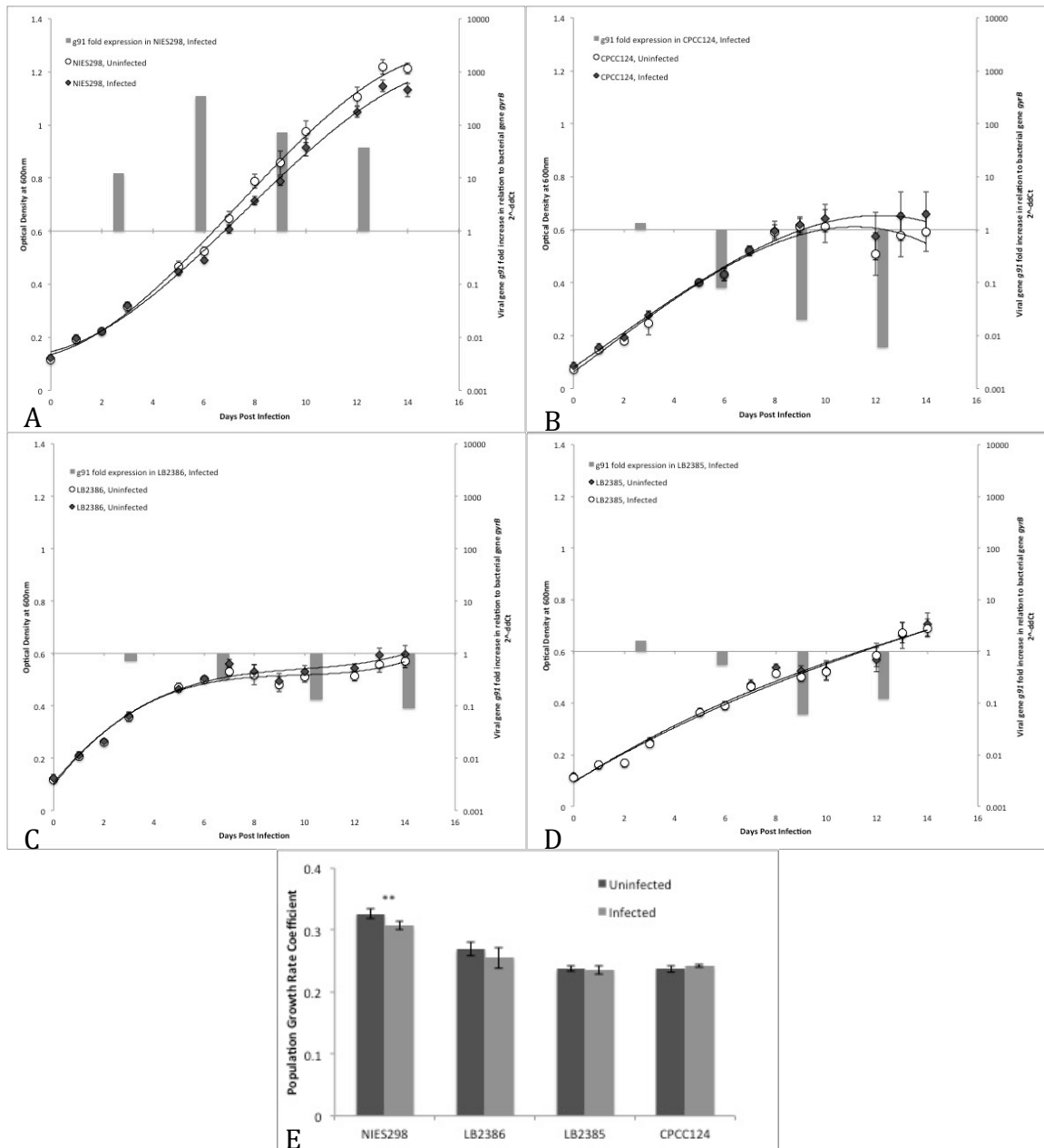


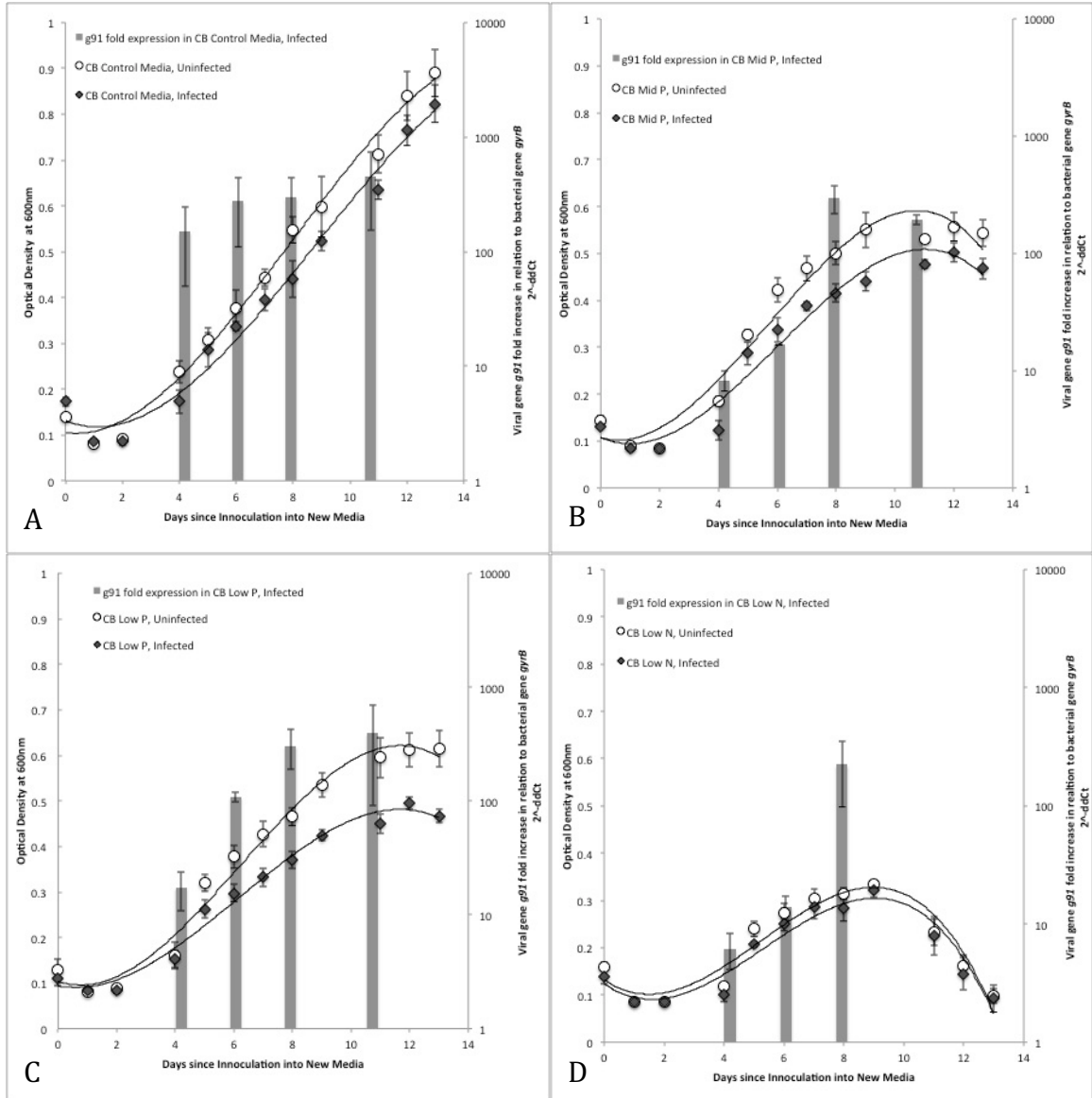
Figure 8. Host specificity test of Ma-LMM01 on North American Strains of *Microcystis aeruginosa* CPCC124, LB2385, and LB2386. Six replicate cultures of each infected (black diamonds) and uninfected (white circles) were monitored for a period of 13 days. **A.** Growth curve and successful viral infection, as determined by an increase in viral genomes, on NIES298 which is the only known host for the phage. **B.** Infection of the phage on CPCC124, the only north american uni-algal strain used in this study. The negative viral gene numbers indicate an unsuccessful infection. **C.** Infection of the phage on LB2386, which does not allow for viral genome replication. **D.** Infection of the phage on LB2385, which does not allow for viral genome replication. **E.** Growth rates of each strain tested. The only strain with significant differences between the infected ( $0.307 \pm 0.007$ ) and uninfected ( $0.326 \pm 0.007$ ) samples is NIES298 ( $p < .01$ ). LB2386 infected ( $0.256 \pm 0.017$ ) and uninfected ( $0.270 \pm 0.11$ ), LB2385 infected ( $0.236 \pm 0.007$ ) and uninfected ( $0.238 \pm 0.004$ ), and CPCC124 infected ( $0.242 \pm 0.002$ ) and uninfected ( $0.237 \pm 0.005$ ) are not statistically different. Error bars represent standard deviation of six replicate culture tubes.

### 3.6 Nutrient Stress Infection Trials

To understand how a viral infection of *M. aeruginosa* works under decreased concentrations of nitrogen and phosphorus, as can be seen in a cHAB, we tested growth in nutrient replete media, mid phosphorous (1.53% of CB control), low phosphorus (0.7% of CB control), and low nitrogen (26.55% of CB control) (Table 4). These nutrient-limited conditions can be related to the average yearly concentration of phosphorus in the western basin of Lake Erie, which ranges from 0.05–0.5 mg/L (US EPA, 2015). The mid-phosphorus media modifications are in the middle of this range, while the low-phosphorus media modifications are at the low end of this range.

In nutrient replete media, the growth rate and carrying capacity was lowered slightly in the infected sample in comparison to the uninfected sample (Figure 9A), which was consistent to the trends seen in Yoshida et al. (2014). The samples reached late log on days 13–14, and did not quite reach stationary phase, reading 0.9 OD (600 nm). The viral genome was replicated within 4 days, and reached a maximum at about a 400-fold increase. In the mid phosphorus media, there was a decrease in the carrying capacity of the population due to nutrient limitation, as seen in the uninfected samples compared to the uninfected samples in nutrient replete media (Figure 9A, 9B). The growth of the uninfected samples reached stationary phase at 0.6 OD (600 nm), and the infected samples reached stationary phase at 0.5 OD (600 nm). The viral genome replication took longer to reach maximum replication than the nutrient replete infection by not reaching about a 300-fold increase until day 8, and having a more step-wise increase leading up to it, which might be related to a delayed onset of infection (Figure 9B). This viral relationship is mirrored in the low phosphorus media samples: a step-wise increase of

viral genomes until day 8, in which the maximum viral replication is obtained at about a 400-fold increase from day 0 (Figure 9C). Of note is that there is now a larger difference in growth patterns between the infected and uninfected samples in the low phosphorus media. The carrying capacity of the infected population was lower, and the growth was slower. In the final nutrient modification, the concentration of nitrogen was limited (Figure 9D). When nitrogen was lowered, the host did not grow well, reaching stationary phase at 0.4 OD (600 nm) and declining into the death phase within two days. It appears that there was not much of a difference between the growth patterns of the infected and uninfected samples in the nitrogen limited media, but the virus did replicate its genome by day 8, and reached the viral replication max of about a 300-fold increase from day 0, a viral trend that was seen in all nutrient modifications this trial.



We then calculated the actual values for the carrying capacity and growth rate coefficient using a non-linear regression analysis and performing ANOVA on the resulting averages (Figure 10). There was a significant difference in the growth rate between the infected and uninfected samples in the nutrient replete media ( $p < .01$ ), mid phosphorus media ( $p < .05$ ), and low phosphorus media ( $p < .001$ ) (Figure 10A). The uninfected growth rates for all phosphorus modified media and the nutrient replete media were not statistically different, but the carrying capacities were (Figure 10B). This suggests that until the phosphorus was used up, the host grew at a steady rate ( $r = 0.225$ ), but once nutrient is limited the host stopped replication, leading to a lower carrying capacity. In the infected samples, there was no statistical difference between the growth rate in the nutrient-replete media and the mid-phosphorus media, but a difference was observed in the low phosphorus infected growth ( $p < .01$ ), which was lower than both the mid-phosphorus and nutrient-replete infected growth rates (Figure 10A). In the low nitrogen samples, there was no statistical difference between the carrying capacity of the populations (Figure 10B), but there was a statistical difference between the growth rates between the infected and uninfected ( $p < .01$ ) (Figure 10A).

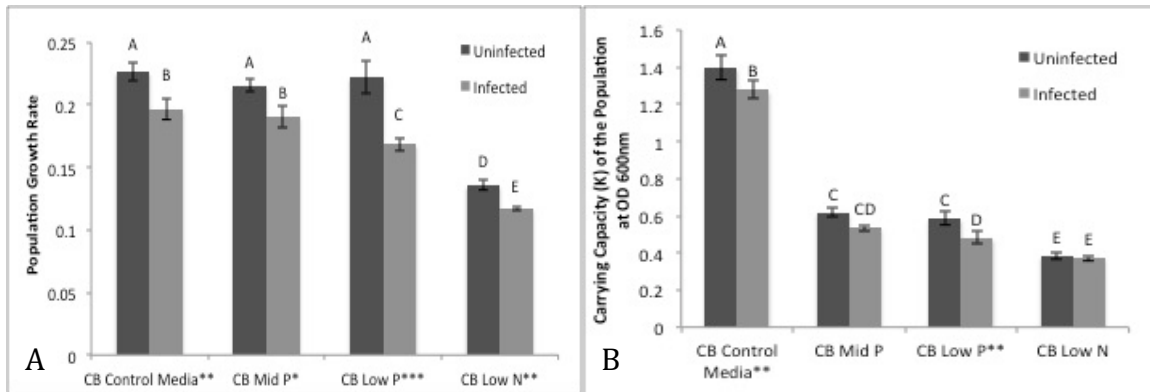


Figure 10. Trial 1: Growth rate and carrying capacity of each media. (\* =  $p < .05$ , \*\* =  $p < .01$ , \*\*\* =  $p < .001$ ) **A.** Population growth rates vary depending on the media, but within each media, there is a statistical difference between the growth rates of the infected and uninfected populations. Specific growth rate coefficients are as follows: CB control uninfected ( $0.226 \pm 0.007$ ) and infected ( $0.197 \pm 0.008$ ), CB Mid P uninfected ( $0.215 \pm 0.004$ ) and infected ( $0.190 \pm 0.008$ ), CB Low P uninfected ( $0.222 \pm 0.013$ ) and infected ( $0.168 \pm 0.005$ ), CB Low N uninfected ( $0.136 \pm 0.003$ ) and infected ( $0.117 \pm 0.002$ ). **B.** The carrying capacity of the populations drops when grown on modified media. Specific carrying capacities are as follows: CB control uninfected ( $1.399 \pm 0.067$ ) and infected ( $1.278 \pm 0.049$ ), CB Mid P uninfected ( $0.619 \pm 0.026$ ) and infected ( $0.535 \pm 0.017$ ), CB Low P uninfected ( $0.587 \pm 0.036$ ) and infected ( $0.481 \pm 0.034$ ), CB Low N uninfected ( $0.382 \pm 0.017$ ) and infected ( $0.371 \pm 0.014$ ).

In a second trial, Ma-LMM01 infections were conducted within the nutrient-limited media (Table 4), without prior centrifugation of the cells. This was done to examine the effect of the nutrient availability for infection rate, specifically the attachment and absorption of the phage. In the nutrient replete and phosphorus modified media samples, the host took a longer time to replicate initially, leading to a delayed exponential phase and a slower overall growth rate than seen in previous trials (Figure 11). In nutrient replete media, the phage genome replicated within 9 days, and reached about a 200-fold increase (Figure 11A). Viral replication also occurred in both phosphorus-limited media, reaching about a 100- to 200-fold increase (Figure 11B, 11C). Of note are the low-phosphorus modified media infected samples, in which viral replication occurred as the culture appeared to reach late-logarithmic growth phase, and by day 9, reached a maximum fold replication similar to the levels seen in the first trial (Figure 9C, 11C). The initial viral replication occurred much later than the first trial but



reached 400-fold increase by day 9 (compared to day 8 in the first trial). Additionally, there appears to be a difference in the growth patterns between the infected and uninfected samples in the low-phosphorus samples, but because the uninfected samples did not reach stationary phase, the statistical comparison was not completed. We did not see the stationary phase of most of the samples, with the exception being the low nitrogen samples (Figure 11D) and the infected low phosphorus samples (Figure 11C). Growth in the low nitrogen samples was similar to that seen in the first trial, in which the growth reached stationary phase by day 7 at 0.4 OD (600nm), and quickly died off after that. While the growth patterns were similar between the two trials for this nutrient modification, the phage replication was not. In the first trial, we had viral genome replication to about a 200-fold increase from day zero, and in the second trial, we have no positive viral genome replication (Figure 11D), which suggests that nitrogen might be a vital nutrient for viral infection or replication, as well as for bacterial growth.

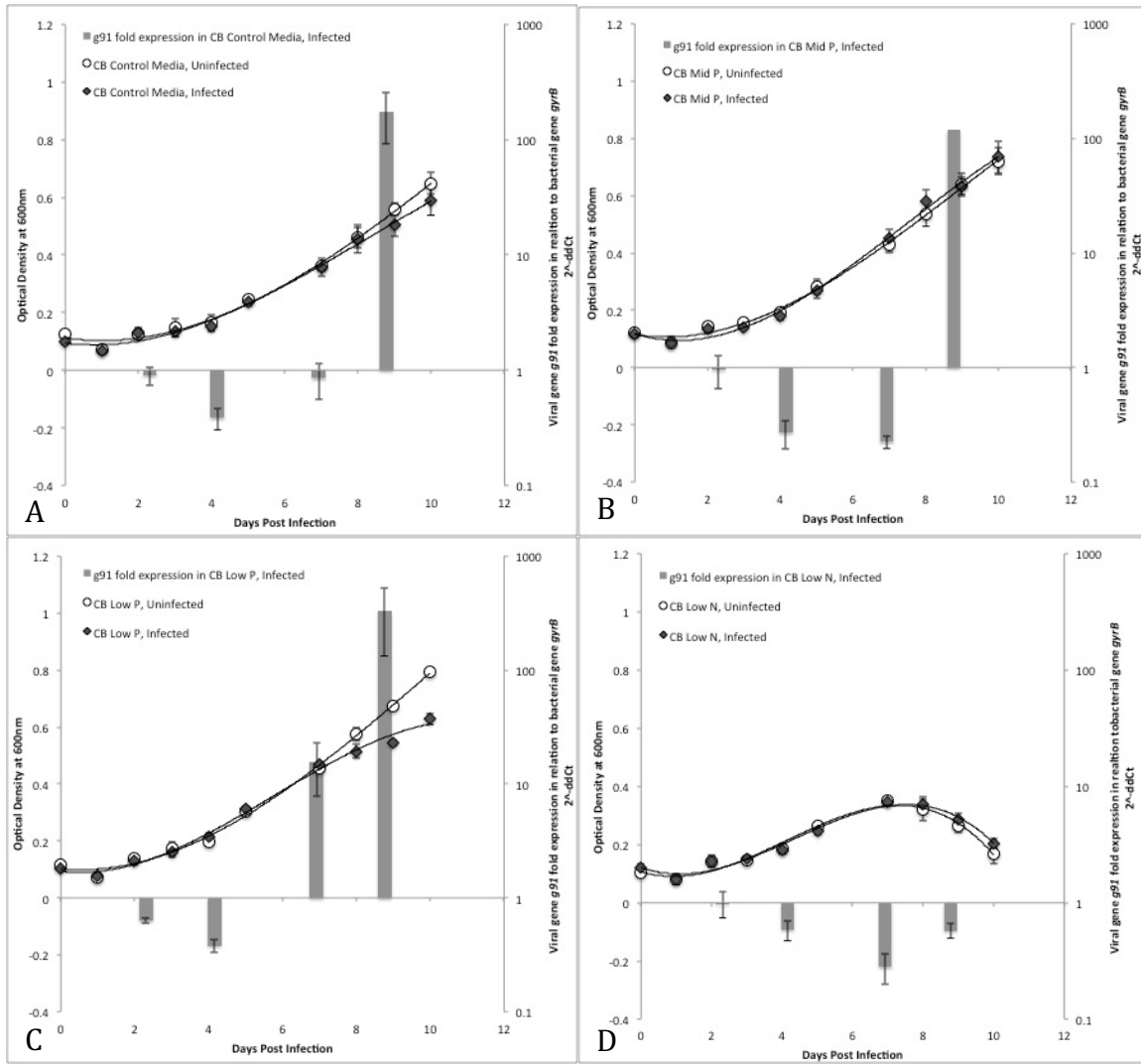


Figure 11. Trial 2: Infection in nutrient-limited media. **A.** Infection in nutrient replete media. The host cells took longer to reach exponential phase in this trial than in the first trial, which correlates to a delayed infection (day 9). **B.** Infection in mid phosphorus modified media (1.53% P of the control), with a delay in infection. **C.** Infection in low phosphorus modified media (0.7% P of the control), with a delay in infection but with similar viral replication quantities to the previous trial. **D.** Infection in low nitrogen modified media (26.55% N of the control). When the phage is inoculated in the limited media, no viral replication occurs.

The third trial was set up in an effort to replicate the negative effect on the growth rate of the host seen between the infected and uninfected samples grown in low phosphorus media in comparison to the difference between the infected and uninfected samples grown in nutrient replete media. The experiment used similar conditions as the first trial, repeated on a larger scale. In this trial, the MOI was about 10-fold less than the previous trials, at 0.008. In the nutrient replete media, infection with the phage did not change the growth of the host (Figure 12A). While an increase in viral genomes was observed, it did not occur in all replicate samples until day 9 and did not reach a maximum level until day 11, much later than previous trials. While the phage replication did not occur until later in the experimental period, the infection reached a higher fold increase compared to the zero point at a 1000-fold increase (10-fold more than previous trials). Because this replication did not occur until later, no differences in growth rate or carrying capacity can be readily seen. As the population reached late logarithmic growth phase, the host cells divided at a slower rate, and since viral replication occurred at this late stage of growth, differences in the growth rate due to the host reaching saturation density and differences in growth rate due to viral replication may be indistinguishable.

In the low phosphorus media, there were no successful infections (Figure 12B). The growth of the uninfected and infected samples overlapped for the whole duration of the experiment, and the viral genome numbers decreased, which is an indication that genome replication did not occur. To be assured that the difference in growth rate was not due to the fact that we lowered both the source of phosphorous and the salt it was bound to, we also tested a media that had sodium added back into the low phosphorus media to create an ion-compensated low phosphorus media (Figure 12C). In this data set, we had

two successful infections and four unsuccessful infections, which have been separated for analysis to determine if there are any differences in the populations. The sample set with the lowest growth curve was the successful infection, while the set with the highest growth curve was the unsuccessful infection. The growth rates of the two populations were statistically different ( $p < .05$ ), but further testing is needed to create an accurate representation of real occurrences (Figure 12D). Of the successful infections, the delay before replication occurs was much shorter than the replete media control, but the fold increase in replication was smaller as well, only reaching 100-fold increase. Since there was viral genome replication in some of the salt adjusted samples, all of the nutrient replete samples, and none of the unadjusted low-phosphorus samples, ionic strength may play a role in the infectivity of the phage.

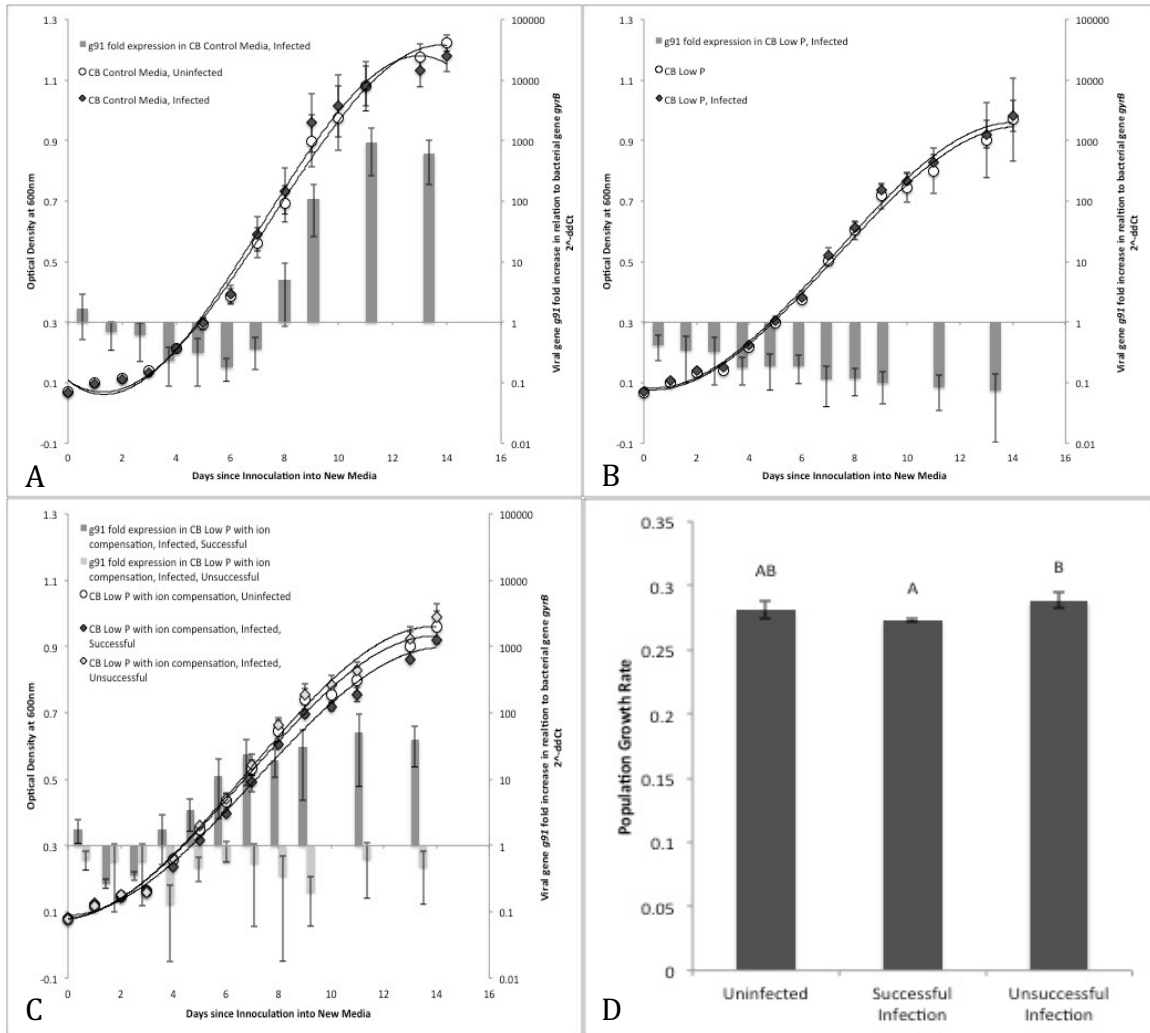


Figure 12. Trial 3: Infection in phosphorus-limited media and phosphorus-limited media with salt compensation. **A.** Infection in nutrient replete media. A lowered MOI caused a delay in infection. **B.** Infection in low phosphorus modified media (0.7% P of the control). No positive viral replication occurred. **C.** Infection in low phosphorus modified media (0.7% P of the control) with ion compensation (added Na). Two samples with positive viral replication and four samples with no positive viral replication were separated and analyzed as two different groups. **D.** Growth rates of the uninfected (0.281±0.007), the successful infection (0.273±0.001), and unsuccessful infection (0.288±0.006) in the low phosphorus modified media with ion compensation.

## Discussion

This study aims to understand how different factors can come together to regulate the composition and longevity of a cyanobacterial Harmful Algal Bloom (cHAB) by focusing on nutrient limitation and phage infection in the prominent freshwater cyanobacterium, *Microcystis aeruginosa*. To this end, we used the characterized *M. aeruginosa*-phage system, *M. aeruginosa* NIES298 and Ma-LMM01, both of which have been isolated from a eutrophic freshwater lake in Japan. Using this system, we tested the hypothesis that a viral infection by Ma-LMM01 will enhance the negative effect phosphorus limitation has on the growth rate and carrying capacity of a *M. aeruginosa* NIES298 population.

### 4.1 Characterization of Viral Infection in NIES298

*Microcystis aeruginosa* has a complex CRISPR-Cas system that allows the host to combat infection by cyanophages over time, which is involved in the evolution of a host-phage relationship. As originally characterized by Yoshida et al. (2006, 2008), the phage Ma-LMM01 is lytic in its host, *M. aeruginosa* NIES298, visibly clearing the culture within a few days (Yoshida et al. 2006), but repeat infections will shift the host population towards resistance as the host acquires post-infection immunity (Yoshida et al. 2014). The strain of NIES298 that was used in this study has characteristics consistent with the isolates of NIES298 that was classified as MaLMM01 intermediate-susceptible, as described in Yoshida et al. (2014). The published isolates caused a viral infection that does not cause clearing of the culture, but does cause a difference in growth rate compared to an uninfected control (Figure 7). According to Yoshida et al. (2014), these intermediate-sensitive isolates continued to show altered growth through multiple

passages, which may indicate that both sensitive and resistant cells co-exist in the culture and that the host cells were not acquiring post-infection immunity. The environmental survival of a phage relies on there being a susceptible host available to support viral replication, but complete susceptibility to a phage will decimate the host population, so resistant host cells are selected for in a viral infection. One of the explanations for this back and forth relationship between a host and its phage is that phage resistance comes at a cost, whether it be a slowed growth rate or an increased susceptibility to another phage. Additionally, they add that there might be a growth rate cost for phage-resistance under direct competition. This growth rate cost can be seen in other host-phage systems, for example marine cyanophages with *Prochlorococcus* genus hosts (Avrani et al. 2011). In *Prochlorococcus*, when challenged with a phage infection, half of the tested populations grew significantly more slowly than the controls, and some populations that grew resistant to one phage were even more susceptible to another phage (Avrani et al. 2011).

In the system presented in this study, the phage-resistance seems to correlate to a decreased growth rate (Figure 7). During Ma-LMM01 infection, the growth rate of the infected cultures is different than that of the uninfected cultures (Figure 7A-B), but complete lysis of the culture does not occur. Assuming that there is stability in the host housekeeping transcript *gyrB*, the viral genome is being replicated as indicated by an increase in the quantity of the single-copy viral gene *g91*. We use a relative increase in the viral gene *g91* compared to the single-copy bacterial gene *gyrB* as a proxy for replication of the viral genome, per Livak and Schmittgen's (2001) work on the  $2^{-\Delta\Delta C_t}$  equation. Consistent with a viral infection with a replicating virus, we see an increase in viral genomes over a few days and then a leveling off of the relative value (Figure 4A,

6A). According to Yoshida et al. (2014), in the intermediate-susceptible stains, a portion of the population is susceptible to the phage, and another portion of the population is resistant to the phage. If this is the case, then the susceptible population is infected within a few days, and the viral genome is replicated. Once that population has been completely infected, there are no other susceptible cells to infect, and the phage cannot replicate its genome further.

What is still unclear is what happens once the genome has been replicated. When the DNA was isolated from cell samples that had been washed three times with DI water, the viral genes in the sample are associated with the cells (Figure 7C), indicating that once the genome is replicated, the virus remains associated with the host cell. This result could indicate that the method used to wash the cells was not sufficient to separate free virus from the pelleted cells, that the phage has some latent infection properties, or that the host has activated some defense genes and the phage has undergone an abortive infection. Testing the supernatant or running the experiment again with a *DNase* treated negative control in future studies would give us a better understanding of the cell-associated viral signal, while additional experiments would be required to test the other two hypotheses.

The consistent replication between the host *gyrB* and the viral *g91* in the later portion of the infection (in which the proportion of *g91* to *gyrB* is maintained) could be indicative of a lysogenic phage. Because the phage is quantitated relative to a control gene found in the bacteria (*gyrB*, a single copy housekeeping gene), as the host continues to grow, we would expect the proportion of viral genes to bacterial genes to decrease slightly. During a normal lytic infection, a phage (or a few) will infect a host and modify



the host's replication and transcription processes in order to create progeny phage. The lytic life cycle occurs quickly, where most of the susceptible hosts will be infected within a few days. In the case of a lysogenic cycle, we would expect the phages to infect the susceptible hosts and integrate into the host genome, replicating at the same rate as the host replicates. In this case, the genome data would show a consistent ratio of phage to host genes as the phage and host replicate together. What was observed in this data set was that after an increase of phage genomes, the proportion of phage to host genes maintains itself overtime, suggesting that the phage genomes are still increasing and at a rate constant with the growth rate of the host.

While the literature states that Ma-LMM01 is a lytic phage, it has some molecular homologues of lysogeny. Ma-LMM01 has the genes for two prophage anti-repressors that are important in the regulation of lytic and lysogenic cycles (Yoshida et al. 2008; Yoshida-Takashima et al. 2012). For example, in lambdoid phage family, there is a lysogenic phage N15 in which the prophage antirepressor *antC* is active under cellular stress response, specifically DNA damage, which causes the phage to enter the lytic cycle (Mardanov and Ravin 2007). In addition to the two prophage antirepressors, Ma-LMM01 also has the genes for a site-specific recombinase homologue and a flanking transposase gene homologue, which are frequently used by temperate phages to integrate the phage genome into the bacterial chromosome (Groth and Calos 2004). Kuno et al. (2010) rename these two gene homologues IS607-cp; the first gene is in the serine recombinase family of site-specific recombinases, and the second gene is a transposase gene, but the authors note that its transposition activity remains unclear. Further analysis of related strains of *M. aeruginosa* to NIES298 reveals that IS607-cp is present in NIES90, which

was isolated from the same lake (Lake Mikata) as NIES298 and Ma-LMM01. This finding suggests that Ma-LMM01 may have not always been so strain-specific when it comes to a host. NIES90 is not known to be susceptible to Ma-LMM01, but it was hypothesized that phage mediated transfer of these elements can occur (Kuno et al., 2010).

While a latent infection is a possible explanation, another possible interaction between the intermediate-sensitive strain of NIES298 and the cyanophage Ma-LMM01 is related to the complex immune system found in *M. aeruginosa*. In the fully sequenced genome of *M. aeruginosa* NIES843, there are 492 defense genes identified, which correlates to about 29% of its genome being related to defense islands (Makarova et al. 2011). Included in these defense islands are genes that encode for restriction-modification systems (RM), toxin-antitoxin systems (TA), and the abortive infection (ABi) system. All of these systems stops phage infection at different stages such as replication, transcription, or translation, and can lead to the death of the infected cell (Makarova et al. 2011). If the phage has been stopped by any of the host's defense genes, then we could get successful replication of the phage genome, but no formation of complete new virus particles. Additionally, the cell death caused by the host defense system may lower the number of *gyrB* copies in the sample, which may explain the consistent relative relationship between *g91* and *gyrB*.

#### 4.2 Testing for North American Strains of *M. aeruginosa* for Ma-LMM01 Susceptibility

Lake Erie contains an estimated  $0.3\text{--}4.1 \times 10^8$  virus-like particles per mL (DeBruyn et al. 2004). These viruses can have hosts in the numerous heterotrophic bacteria, protozoa, or phytoplankton families found in Lake Erie, and they play a role in

the normal regulation of the freshwater ecosystem. Because of the large number of virus-like particles in the environment, it is assumed that there is a phage specific for every possible host. *M. aeruginosa* is found in numerous freshwater lakes in Northern America, so we wanted to test the most characterized cyanophage specific for *M. aeruginosa* on different North American strains (Table 1, Figure 8).

Prior to infection with Ma-LMM01, the North American strains of *M. aeruginosa* were analyzed for the presence of the viral genes *g91* (a sheath protein) and *nbla* (an early viral gene, responsible for a phycobilisome degradation protein) (Table 2, Figure 6). The viral gene *g91* is specific for *M. aeruginosa*-infecting cyanophages (Xia et al. 2013) while *nbla* was originally a host gene that was responsible for the recycling of the phycobilisome, or major photosynthetic complex of pigmented proteins, in a number of phytoplankton species, including *Synechococcus* and *Anabaena* (Karradt et al. 2008). After electrophoresis of the *g91* amplimers from each host (Figure 6), there are a few bands amplified from the *g91* primers, and many amplified products using the *nbla* primers. For *g91*, bands occur at < 500 bp in CPCC124, a unialgal strain, and in LB2386 and LE3, both mixed algal cultures. Since the bands are so much larger than the control viral gene and the fact that most of the bands were seen in mixed algal cultures, we do not believe the presence of these bands is an indication of an active lysogenic infection, but may be non-specific binding to a different bacterial gene, as indicated by the melting curve analysis of the product (data not shown). Sequencing of these bands in the future would give us further information about the specificity of the *g91* primers. For *nbla*, we have bands close in size to the viral *nbla* control (Figure 6) in CPCC124, LB2386, LB2385, and LE3. Additionally, there are a number of bands < 500 bp in every strain but

NIES44. Similar to the large bands for *g91*, the bands greater than 500 bp are likely due to primer binding to a different bacterial gene, but the bands that are close in size to the viral *nblA* control may be homologues to the original *nblA* that the phage had acquired from its host, or they may indicate the presence of integrated viral genes in the host genome in the form of a prophage. In order to make any conclusions about the origin of the close sized *nblA* bands, sequencing would be required.

Because of the uncertainty in origin of the *nblA* bands, only *g91* was used to quantitate the virus in the host specificity test. The only viral amplification that occurred was in *M. aeruginosa* NIES298, which also had the only significant difference in growth rate between the infected and uninfected samples (Figure 8). These data support the idea put forward by Yoshida et al. (2006) that stated that Ma-LMM01 has a narrow host range, which is only *M. aeruginosa* NIES298. The specificity of a single strain for a host is unusual for a phage, and even unusual for phages in the Cyanomyoviridae family (Xia et al. 2013). Two other phages from this family, AS-1 and N-1, are not as limited in their host range, where AS-1 can infect unicellular freshwater cyanobacteria *Anacystis* and *Synechococcus* (Safferman et al. 1972), and N-1 can be lytic or lysogenic some strains of *Nostoc* and *Anabaena* (Adolph and Haselkorn 1971; Currier and Wolk 1979). Perhaps the specificity of Ma-LMM01 allows it to co-evolve more efficiently with its host and combat its host immune system better, but the relationship requires further study.

#### 4.3 Combined Effect of Nitrogen Limitation and Viral Infection

Unlike many cyanobacterial species, *M. aeruginosa* does not have the capability to fix nitrogen, but continues to dominate some blooms when the nitrogen to phosphorus ratio was low (Fujimoto et al. 1997). In the comparison of the nitrogen-limited media in

the first trial (Figure 9), in which *M. aeruginosa* had been infected in replete media for 24 hours before the cells were spun down and suspended in low nitrogen media, and the nitrogen-limited media in the second trial (Figure 11), in which the cells were inoculated in the nutrient-limited media, and then infected, there is a large difference in viral replication. When allowed to incubate in replete media, the virus attaches and replicates efficiently, as seen in both the nutrient-replete and phosphorus-limited samples of the first trial. The similar ratio of viral replication suggests that even in nitrogen-limited stress, the phage does not have trouble reaching full genome replication in the host. When the phage is placed in the nitrogen-limited media, no positive replication occurs, suggesting that nitrogen might be important in phage absorption. Unfortunately, there is not much literature current that addresses the effect of nitrogen on cyanophage infection.

The nitrogen content of the waters in which *M. aeruginosa* is found is vital for the daily activities of the cell, as it is an essential nutrient in protein (which includes cell surface receptors, transport systems, and nutrient-scavenging systems) and DNA synthesis. Nitrogen concentrations have also been linked to the cyanobacteria's ability to produce microcystin and cellular buoyancy. While the decreased production of Microcystins under nitrogen limitation (Vezie et al. 2002) may not be related to phage infection, the changes in cell morphology might. When nitrogen is depleted in a system, *M. aeruginosa*'s gas vesicle volume is decreased to the point that the host can no longer remain buoyant (Brookes and Ganf 2001). Characteristically, cyanophage production depends on host photosynthesis, which occurs with a diurnal pattern (Kao et al. 2005). Ma-LMM01 is like other characterized cyanophages in this respect: in the field, Ma-LMM01 phage genomes peak during daylight hours and are at their lowest values late at

night (Kimura et al. 2012). If the phage requires host photosynthesis to propagate, and the host must be able to regulate buoyancy to be fully photosynthetic, then changes in host buoyancy would affect the propagation of the phage. In this instance, the phage may encounter and attach to the host cell, but it would not be able to replicate its DNA. In the first trial, the cells were infected in nutrient replete media, which would have allowed attachment of the phage. Transfer into nutrient replete media may allow the phage time to initiate replication of the viral genome prior to complete nitrogen limitation (Figure 9D). Infection in nitrogen-limited media does not allow the phage much time to initiate viral replication prior to host nitrogen limitation (Figure 11D).

While there is evidence that nitrogen is a vital nutrient for *M. aeruginosa* blooms (Lopez et al. 2008; Paerl et al. 2011; Paerl and Otten 2013; Zhu et al. 2015), there is still very little information about the combined effect of nitrogen limitation and viral infection on any cyanobacterial species, not just *M. aeruginosa*. Further work should continue to establish the relationship between limiting nitrogen in the environment and phage propagation.

#### 4.4 Combined Effect of Phosphorus Limitation and Viral Infection

Under normal conditions, many freshwater lakes are phosphorus limited (Smith 1983), and therefore, the increased phosphorous run off from agricultural, residential, and industrial practices has been blamed for the increased prevalence of cHABs. A number of cyanobacteria species have a suite of genes that encode for proteins that increase phosphorus assimilation under low phosphorus conditions called *Pho* genes; these genes have been selected for due to the normally limited phosphorus availability of the cyanobacteria's environment (Vershina and Znamenskaya 2002). These *Pho* genes

include phosphate-binding proteins such as *pstS* (ABC-type phosphate transport system) and hydrolysis proteins such as *phoA*, both of which can be found in *M. aeruginosa* (Harke et al. 2012). In addition to being present in the host, there are a number of cases where these two genes have been present in cyanophage genomes. Homologues for *pstS* were found in nine of 16 cyanophages isolated on *Prechlorococcus* and *Synechococcus* host strains, all of which were isolated from low-nutrient waters. Two of these phages also encoded *phoA*, which facilitates the phage's access to organic phosphorus (Sullivan et al. 2005, 2010). The presence of these genes in both the cyanophage and the host is a function of environmental phosphate availability (Kelly et al. 2013). These genes likely have a role in phage DNA replication by facilitating host phosphorus acquisition during infection. Phage infection in *Synechococcus* under phosphorus stress up regulates the host's phosphate acquisition genes, which allow the cell to continue to acquire phosphorus during the infection; the phosphorus could then be used in phage DNA replication and the building of virus particles (Lin et al. 2016). When *M. aeruginosa* encounters low phosphorus stress, these *pho* genes are activated, which allows the cells to persist.

The effect of phosphorus limitation on *M. aeruginosa* alone can be seen in the comparison of growth parameters in the first trial of nutrient limitation tests (Figure 9). The nutrient replete uninfected sample represents the best possible growth that the cells can achieve given the simulated environmental conditions with no nutrient stress or outside competition. In both the mid-level phosphorus and the low-level phosphorus uninfected samples, the growth rates are not significantly different from each other. Phosphorus limitation alone does not alter the growth rate, but it does signal to the cells

to stop dividing earlier (Figure 10). The carrying capacity for the mid- and low-level phosphorus media was much lower than the replete media but was not much different from each other, which suggests that infection with the cyanophage allows the host to acclimate to varying levels of diminished phosphorus the same.

In the second trial, the infection occurred in the modified nutrient media. Instead of seeing the effects of phage replication on the host while the host is undergoing phosphorus limited stress, this trial examines the ability of the phage to attach and be absorbed into the host under mid- and low-phosphorus conditions (Figure 11). Despite the delayed infection in the nutrient replete, mid-level, and low-level phosphorus media, there is still positive amplification of viral genomes as seen by an increase *g9I* genes, which indicates the phage has successfully attached to and entered the host to the point of genomic replication. The maximum level of *g9I* is similar between the three media types, which again seems to suggest that the phosphorus limitation does not greatly alter the ability for the phage to replicate.

The third trial was designed to examine the reproducibility of the nutrient-limited differences in cyanobacterial growth rates and to ensure that the differences seen in previous trials were due to nutrient limitation. Particularly, we re-analyzed the difference seen between the nutrient-replete media and the low-level phosphorus media infected samples to show that there was a repeatable decrease in host growth rate when nutrient limitation and viral infection stress were combined. To ensure that the nutrient limitation was the only controllable variable, this trial compensates for the removal of sodium. Historically, when *M. aeruginosa* is studied in the context of nutrient limitation, the nutrient in question is removed, and the accompanying salt is not compensated for in the



modified media (Fujimoto et al. 1997; Downing et al. 2005; Zhu et al. 2015). Some phages require a certain amount of divalent cations for phage adsorption and early viral replication, like calcium and magnesium (Roundtree and Freeman 1955; Puck 1953), so the re-addition of salt was included as a control.

The third trial had a decreased MOI, which has led to a delay in viral replication. In the nutrient replete media, viral replication does not occur until the host has reached late log phase, and no difference in growth rate can be seen (Figure 12). While viral replication occurs late in the experiment, it reaches the same relative level as seen in the first trial. These data are consistent with the idea that a percentage of the population is susceptible to the phage, and once that population has been infected, the phage does not replicate in the resistant population. The viral infection was completely unsuccessful in the low-phosphorus media, which may indicate that there is a minimal viral threshold in which the infection is possible in low-phosphorus stressed cells. In the low-phosphorus ion compensated media, two infections were successful and four were not. The two positive infections indicate that the MOI was close to the dilution in which viral infection does not occur. Of the two successful infections (Figure 12), viral replication occurs by day 4, and increases in a step-wise function to day 9, which is the viral replication trend seen in the low-phosphorus samples from the first trial (Figure 9). While the increase in viral genes is similar, the fold-increase in viral genomes is 5- to 10-fold less in the third trial compared to the amplification seen in other trials (Figure 9, Figure 11, Figure 12). A decrease in viral replication would create less of a strain on the host, which would correlate to a closer growth rate to the uninfected samples.

Combined, these trials present the idea that while both phosphorus limitation and viral infection are stressors on the host cell individually, when combined, they work together to decrease the ability of the host to divide (growth rate and carrying capacity of the population decrease). The mechanism behind the difference in growth is unclear, but it may be related to the fact that Ma-LMM01 has an ORF that shows significant sequence similarity to *E. coli phoH*, which is an ATPase induced under phosphate starvation (Yoshida et al. 2014). *phoH* is a cytoplasmic protein that belongs to the Pho regulon, which regulates phosphate uptake and metabolism under low-phosphate conditions. *phoH* is the most commonly found Pho regulon gene found in phages of both marine and terrestrial environments, and the gene has been found in both heterotrophic- and autotrophic-infecting phages (Goldsmith et al. 2011). The exact function of this homolog is unclear, but it is likely related to regulation of the host *pho* system described above.

Another potential mechanism behind the decreased growth rate of the populations of *M. aeruginosa* seen when the cells are both phosphate stressed and infected is due to viral lysogeny. When infected by one of its phages, S-PM2, the oceanic cyanobacteria species *Synechococcus* is lysed. When compared to an infection in phosphate-depleted media, the host had a delay in lysis (18 hours) and at a much smaller percent of the population (9.3% in phosphate limited vs. 100% lysis in nutrient replete media). Further study revealed that this phage undergoes lysogeny in response to phosphate stress in the host cell (Wilson et al 1996). This may be advantageous for the phage in instances where the likelihood of coming in contact with another host is reduced (Wiggins and Alexander 1985), such as instances of low nutrient availability in which the host is not rapidly expanding. Additionally, lysogenized cells can also benefit by gaining access to genes

carried by the virus (such as up-regulation of phosphate stress genes) (Waldor and Mekalanos 1996). Continuing work on the potential lysogeny of wild cyanophages shows that most lysogenic phages enter the lysogenic phase during periods of low water temperature, rainfall, nutrient concentration, and bacterial productivity, which are conditions that are not favorable for the host bacterial growth and production (Williamson et al. 2002). This study goes on to note that decreases in phosphorus concentrations contribute to potential lysogeny (as tested by induction of prophages with mitomycin C), while elevated levels of nitrogen shift the relationship towards lytic infections (Williamson et al. 2002). It is worth noting that while lysogeny has not been seen in this particular host-phage system, lysogeny has been confirmed in a strain of *M. aeruginosa* isolated from South East Queensland, which had a 99% lysogenic fraction based on their calculated burst size (Steenhauer et al. 2014).

Phosphate stress is a significant regulation factor of cHABs, as indicated by the presence of many phosphate-stress inducible genes found in both cyanophages and their hosts. Further study would explore the relationship between Ma-LMM01 *phoH* and the potential activation of the host *Pho* genes under phosphorus stress by monitoring *pho* transcription during phage infection. Additional work could also analyze potential lysogeny of Ma-LMM01 on *M. aeruginosa* under long-term phosphate stress, or further isolate both lytic and lysogenic phages from local water sources at various time points throughout the year.

## Conclusion

Based on the trials we ran, our data supports the hypothesis that the cyanophage will have a greater negative effect on the growth properties of the host as phosphorus becomes more limited. As mentioned before, this relationship does not appear to affect the replication of the phage, just the host. The growth rate of *M. aeruginosa* is affected by infection, and the carrying capacity of the population is affected by phosphorus limitation; when combined, the data suggests that the phage infection slows the growth of the hosts while potentially increasing the host's phosphate scavenging ability. Practical applications could include future regulation of toxic cyanobacterial species within a cHAB, limiting total cell capacity of a cHAB, or even limiting the duration of a cHAB. In particular, this work suggests that a viral infection under low phosphorus conditions would yield the best results in controlling some species in a cHAB.

Additionally, this work searches for other potential hosts for the cyanophage Ma-LMM01 using North American strains of *M. aeruginosa*, which was unsuccessful, and introduces a method for restriction digest identification of these strains. Finally, we also introduce a potential relationship between nitrogen availability and cyanophage propagation, in particular, the need for nitrogen in the early stages of viral attachment and absorption.

The next step for this research is to establish if the trends seen here are indicative of real world events. Samplings from Lake Erie at different times during a cHAB can be combined with real-time data about the nutrient concentrations of the lake to establish nutrient and cyanobacterial fluctuations in a freshwater cHAB. That data would give us an idea of actual variations in select cyanobacteria strains and Ma-LMM01-like phages in

terms of differing phosphorus and nitrogen concentrations. Further research about cHABs is important because they are an economic and environmental problem that requires monitoring and control. In order to control cHABs, we have to understand how many of the abiotic and biotic factors work together to regulate the blooms.

## Literature Cited

- Adolph K, Heseltorn R. Isolation and characterization of a virus infecting the blue-green alga *Nostoc muscorum*. *Virology* 1971; 46:200-208.
- Avrani S, Wurtzel O, Sharon I, Sorek R, Lindell D. Genomic island variability facilitates *Prochlorococcus*-virus coexistence. *Nature* 2011; 474:604-608.
- Baier K, Lehmann H, Stephan D, Lockau W. *NbIA* is essential for phycobilisome degradation in *Anabaena* sp. strain PCC 7120 but not for development of functional heterocysts. *Microbiology* 2004; 150:2739–2749.
- Brookes J, Ganf G. Variations in the buoyancy response of *Microcystis aeruginosa* to nitrogen, phosphorus and light. *Journal of Plankton Research* 2001; 23:1399-1411.
- Butler N, Carlise J, Linville R, Washburn B. Microcystins: A brief overview of their toxicity and effects, with a special reference to fish, wildlife, and livestock. Office of Environmental Health Hazard Assessment. California Environmental Protection Agency. 2009.
- Chen F, Lu J. Genomic sequence and evolution of marine cyanophage P60: a new insight on lytic and lysogenic phages. *Applied and Environmental Microbiology* 2002; 68:2589-2594.
- Currier T, Wolk P. Characteristics of *Anabaena variabilis* influencing plaque formation by cyanophage N-1. *Journal of Bacteriology* 1979; 139:88-92.
- Davis T, Watson S, Rozmarynowycz M, Ciborowski J, McKay M, Bullerjahn G. Phylogenies of microcystin-producing cyanobacteria in the lower Laurentian great lakes suggest extensive genetic connectivity. *PloS one* 2014; 9:e106093.
- DeBruyn J, Leigh-Bell J, McKay M, Bourbonniere R, Wilhelm S. Microbial distributions and the impact of phosphorus on bacterial activity in Lake Erie. *Journal of Great Lakes Research* 2004; 20:166-183.
- Deng L, Hayes P. Evidence for cyanophages active against bloom-forming freshwater cyanobacteria. *Freshwater Biology* 2008; 53:1240-1252.
- Downing T, Sember C, Gehringer M, Leukes W. Medium N:P ratios and specific growth rate modulate microcystin and protein content in *Microcystis aeruginosa* PCC7806 and *M. aeruginosa* UV027. *Microbial Ecology* 2005; 49:468-473.

Fujimoto N, Sudo R, Sugiura N, Inamori Y. Nutrient-limited growth of *Microcystis aeruginosa* and *Phormidium tenue* and competition under various N:P supply ratios and temperatures. *Limnology and Oceanography* 1997; 42:250-256.

Gilbert P, Anderson D, Gentien P, Graneli E, Sellner K. The global complex phenomena of harmful algal blooms. *Oceanography* 2005; 18:136-147.

Goldsmith D, Crosti G, Dwivedi B, McDaniel L, Varsani A, Suttle C, Weinbauer M, Sandaa R, Breitbart M. Development of *phoH* as a novel signature gene for assessing marine phage diversity. *Applied and Environmental Microbiology* 2011; 77:7730-7739.

Groth A, Calos M. Phage integrases: biology and applications. *Journal of Molecular Biology* 2004; 335:667-678.

Guillard R. Counting slides. In: A. Sournia (ed.) *Phytoplankton Manual*. UNESCO: Paris, pp. 182-189. 1978.

Harke M, Berry D, Ammerman J, Gobler C. Molecular response of the bloom-forming cyanobacterium, *Microcystis aeruginosa*, to phosphorus limitation. *Microbial Ecology* 2012; 63:188-198.

Honda T, Takahashi H, Sako Y, Yoshida T. Gene expression of *Microcystis aeruginosa* during infection of cyanomyovirus Ma-LMM01. *Fisheries science* 2014; 80:83-91.

Humphries S, Wijaya F. A simple method for separating cells of *Microcystis aeruginosa* for counting. *British Phycological Journal* 1979; 14:313-316.

Kao C, Green S, Stein B, Golden S. Diel infection of a cyanobacterium by a contractile bacteriophage. *Applied and Environmental Microbiology* 2005; 71:4276-4279.

Karradt A, Sobanski J, Mattow J, Lockau W, Baier K. *NblA*, a key protein of phycobilisome degradation, interacts with *ClpC*, a HSP100 chaperone partner of a cyanobacterial Clp protease. *Journal of Biological Chemistry* 2008; 283:32294-32403.

Kasai F, Kawachi M, Erata M, Watanabe M. NIES-collection list of strains, 7<sup>th</sup> ed. The National Institution for Environmental Studies, Tsukuba, Japan. 2004.

Kelly L, Ding H, Huang K, Osburne M, Chisholm S. Genetic diversity in cultures and wild marine cyanomyoviruses reveals phosphorus stress as a strong selective agent. *ISME Journal* 2013; 7:1827-1841.

Kimura S, Yoshida T, Hosoda N, Honda T, Kuno S, Kamiji R, Hashimoto R, Sako Y. Diurnal infection patterns and impact of *Microcystis* cyanophages in a Japanese pond. *Applied and Environmental Microbiology* 2012; 78:5805-5811.

Kuno S, Yoshida T, Kamikawa R, Hosoda N, Sako Y. The distribution of a phage-related insertion sequence element in the cyanobacterium, *Microcystis aeruginosa*. *Microbes and Environments* 2010; 25:295-301.

Kurmayer R, Kutzenberger T. Application of real-time PCR for quantification of microcystin genotypes in a population of the toxic cyanobacterium *Microcystis* sp. *Applied and Environmental Microbiology* 2003; 69:6723-6730.

Lin X, Ding H, Zeng Q. Transcriptomic response during phage infection of a marine cyanobacterium under phosphorus-limited conditions. *Environmental Microbiology* 2016; 18:450-460.

Livak K, Schmittgen T. Analysis of relative gene expression data using real-time quantitation PCR and the  $2^{-\Delta\Delta CT}$  method. *Methods* 2001; 25:402-208.

Lopez C, Jewett E, Dortch Q, Walton B, Hudnell H. Scientific assessment of freshwater Harmful Algal Blooms. Interagency working group on Harmful Algal Blooms, hypoxia, and human health of the Joint Subcommittee on Ocean Science and Technology. Washington, DC. 2008.

Makarova K, Wolf Y, Snir S, Koonin E. Defense islands in bacterial and archaeal genomes and prediction of novel defense systems. *Journal of Bacteriology* 2011; 193:6039-6056.

Mann N, Clokie M, Millard A, Cook A, Wilson W, Wheatley O, Letaroy A, Krish H. The genome of S-PM2, a “photosynthetic” T4-type bacteriophage that infects marine *Synechococcus* strains. *Journal of Bacteriology* 2005; 187:3188–3200.

Mardanov A, Ravin N. The antirepressor needed for induction of linear plasmid-prophage N15 belongs to the SOS regulon. *Journal of Bacteriology* 2007; 189:6333-6338.

Michalak A, Anderson E, Beletsky D, Boland S, Bosch N, Bridgeman T, Chaffin J, Cho K, Confesor R, Daloglu I, Depinto J, Evans M, Fahnenstiel G, He L, Ho J, Jenkins L, Johengen T, Kuo K, Laporte E, Liu X, McWilliams M, Moore M, Posselt D, Richards R, Scavia D, Steiner A, Verhamme E, Wright D, Zagorski M. Record-setting algal bloom in Lake Erie caused by agricultural and meteorological trends consistent with expected future conditions. *PNAS* 2013; 110:6448–52.



Mlouka A, Comte K, Castets A, Bouchier C, Tandeau de Marsac N. The gas vesicle gene cluster from *Microcystis aeruginosa* and DNA rearrangements that lead to loss of cell buoyancy. *Journal of Bacteriology* 2004; 186:2355-2365.

Nakamura G, Kimura S, Sako Y, Yoshida T. Genetic diversity of *Microcystis* cyanophages in two distinct freshwater environments. *Archives of Microbiology* 2014; 196:401-409.

Oh H, Lee S, Jang M, Yoon D. Microcystin production by *Microcystis aeruginosa* in a phosphorus-limited chemostat. *Applied and Environmental Microbiology* 2000; 66:176-179.

Paerl H, Fulton R. Ecology of harmful cyanobacteria. In: Graneli E, Turner J (eds) *Ecology of harmful marine algae*. Springer, Berlin, pp 95–107. 2006.

Paerl H, Xu H, McCarthy M, Zhu G, Boqiang Q, Li Y, Gardner W. Controlling harmful cyanobacterial blooms in a hyper-eutrophic lake (Lake Taihu, China): the need for a dual nutrient (N & P) management strategy. *Water Research* 2011; 45:1973–1983.

Paerl H, Paul W. Climate change: links to global expansion of harmful cyanobacteria. *Water Research* 2011; 46:1349–1363.

Paerl H, Otten T. Harmful Cyanobacterial Blooms: Causes, Consequences, and Controls. *Environmental Microbiology* 2013; 65:995-1010.

Pandan E, Shilo M. Cyanophages-viruses attacking blue-green algae. *Bacteriology Reviews* 1973; 37:343-370.

Puck T. The first steps of virus invasion. *Cold Spring Harbor Symposia on Quantitative Biology* 1953; 18:149-154.

Rapala J, Sivonen K, Lyra C, Niemela S. Variation of microcystins, cyanobacterial hepatotoxins, in *Anabena* spp. as a function of growth stimuli. *Applied and Environmental Microbiology* 1997; 63:2206-2212.

Rodriguez-Valera F, Martin-Cuadrado A, Rodrigues-Brito B, Pasic L, Thingstad T, Rohwer F, Mira A. Explaining microbial population genomics through phage predation. *Nature Reviews Microbiology* 2009; 7:828-836.

Roundtree P, Freeman B. Infections caused by a particular phage type of *Staphylococcus aureus*. *Medical Journal of Australia* 1955; 2:157-161.

Safferman R, Diener T, Desjardins R, Morris M. Isolation and characterization of AS-1, a phycovirus infecting the blue-green algae, *Anacystis nidulans* and *Synechococcus cedrorum*. *Virology* 1972; 47:105-113.

- Shirai M, Matumaru K, Ohotake A, Takamura Y, Aida T, Nakano M. Development of a solid medium for growth and isolation of axenic *Microcystis* strains (cyanobacteria). *Applied and Environmental Microbiology* 1989; 55:2569-2571.
- Sivonen K. Effects of light, temperature, nitrate, orthophosphate, and bacteria on growth of and hepatotoxin production by *Oscillatoria agardhii* strains. *Applied and Environmental Microbiology* 1990; 56:2658-2666.
- Smith V. Low nitrogen to phosphorus ratios favor dominance by blue-green algae in lake phytoplankton. *Science* 1983; 221:669-671.
- Steenhauer L, Pollard P, Brussaard C, Sawstrom C. Lysogenic infection in subtropical freshwater cyanobacteria cultures and natural blooms. *Marine and Freshwater research* 2014; 65:624-632.
- Sullivan M, Coleman M, Weigele P, Rohwer F, Chisholm S. Three Prochlorococcus cyanophage genomes: signature features and ecological interpretations. *PLoS Biology* 2005; 3:e144.
- Sullivan M, Huang K, Ignacio-Espinoza J, Berlin A, Kelly L, Weigele P, DeFrancesco A, Kern S, Thompson L, Young S, Yandava C, Fu R, Krastins B, Chase M, Sarracino D, Osburne M, Henn M, Chisholm S. Genomic analysis of oceanic cyanobacterial myoviruses compared with T4-like myoviruses from diverse hosts and environments. *Environmental Microbiology* 2010; 12:3035-3056.
- Suttle C. Cyanophages and their role in the ecology of cyanobacteria. In: Whitton BA, Potts M (eds), *The ecology of cyanobacteria. Their diversity in time and space*. Kluwer Academic Publishers, Dordrecht, pp 563–589. 2000.
- Tas S, Okus E, Aslan-Yilmaz A. The blooms of a cyanobacterium, *Microcystis cf. aeruginosa* in a severely polluted estuary, the Golden Horn, Turkey. *Estuarine Coastal and Shelf Science* 2006; 68:593-599.
- Tillett D, Neilan B. Xanthogenate nucleic acid isolation from cultures and environmental cyanobacteria. *Journal of Phycology* 2000; 36:251-258.
- Tucker S, Pollard P. Identification of cyanophage Ma-LBP and infection of the cyanobacterium *Microcystis aeruginosa* from an Australian subtropical lake by the virus. *Applied and Environmental Microbiology* 2005; 71:629-635.
- Ueno Y, Nagata S, Tsutsumi T, Hasegawa A, Watanabe M, Park H, Chen GC, Chen G, Yu S. Detection of microcystins, a blue-green algal hepatotoxin, in drinking water sampled in Haimen and Fusui, endemic areas of primary liver cancer in China, by highly sensitive immunoassay. *Carcinogenesis* 1996; 17:1317-1321.

US EPA. Recommended phosphorus loading targets for Lake Erie. Annex 4 Objectives and Targets Task Team Final Report to the Nutrients Annex Subcommittee. 2015.

Vershinina O, Znamenskaya L. The Pho regulons of bacteria. *Microbiology* 2002; 71:497-511.

Vezie C, Rapala J, Vaitomaa J, Seitsonen J, Sivonen K. Effect of nitrogen and phosphorus on growth of toxic and nontoxic *Microcystis* strains and on intracellular microcystin concentrations. *Microbial Ecology* 2002; 43:433-454.

Waldor M, Mekalanos J. Lysogenic conversion by a filamentous phage encoding cholera toxin. *Science* 1996; 272:1910-1914.

Watanabe M, Sawaguchi T. Cryopreservation of water-bloom forming cyanobacteria *Microcystis aeruginosa* f. *aeruginosa*. *Phycological Research* 1995; 43:111-116.

WHO. Algae and cyanobacteria in fresh water. In: *Guidelines for Safe Recreational Water Environments*, pp.136-158. 2009.

Wiggins B, Alexander M. Minimum bacterial density for bacteriophage replication: implications for significance of bacteriophages in natural ecosystems. *Applied and Environmental Microbiology* 1985; 49:19-23.

Williamson S, Houchin L, McDaniel L, Paul J. Seasonal variation in lysogeny as depicted by prophage induction in Tampa Bay, Florida. *Applied and Environmental Microbiology* 2002; 68:4307-4314.

Wilson W, Carr N, Mann N. The effect of phosphate status on the kinetics of cyanophage infection in the oceanic cyanobacterium *Synechococcus* sp. WH7803. *Journal of Phycology* 1996; 32:506-516.

Xia H, Li T, Deng F, Hu Z. Freshwater cyanophages. *Virological Sinica* 2013; 28:253-259.

Yoshida-Takashima Y, Yoshida M, Ogata T, Nagasaki K, Hiroishi S, Yoshida T. Cyanophage infection in the bloom-forming cyanobacteria *Microcystis aeruginosa* in surface freshwater. *Microbes and Environments* 2012; 27:350-355.

Yoshida M, Yoshida T, Kashima A, Takashima Y, Hosoda N, Nagasaki K, Hiroishi S. Ecological dynamics of the toxic bloom-forming cyanobacterium *Microcystis aeruginosa* and its cyanophages in freshwater. *Applied and Environmental Microbiology* 2008; 74:3269-3273.

Yoshida T, Takashima Y, Tomaru Y, Shirai Y, Takao Y, Hiroishi S, Nagasaki K. Isolation and characterization of a cyanophage infecting the toxic cyanobacterium *Microcystis aeruginosa*. *Applied and Environmental Microbiology* 2006; 72:1239-1247.

Yoshida T, Nagasaki K, Takashima Y, Shirai Y, Tomaru Y, Takao Y, Sakamoto S, Hiroishi S, Ogata H. Ma-LMM01 infecting toxic *Microcystis aeruginosa* illuminates diverse cyanophage genome strategies. *Journal of Bacteriology* 2008; 190:1762-1772.

Yoshida T, Kamiji R, Nakamura G, Kaneko T, Sako Y. Membrane-like protein involved in phage adsorption associated with phage-sensitivity in the bloom-forming cyanobacterium *Microcystis aeruginosa*. *Harmful Algae* 2014; 34:69-75.

Zegura B, Gajski G, Straser A, Garaj-Vrhovac V, Filipic M. Microcystin-LR induced DNA damage in human peripheral blood lymphocytes. *Mutation Research* 2011; 726:116-122.

Zhou Y, Chen K, Shi Z, Guo Y, Zhu H, Zhang J, Liu Y. Isolation and identification of the first cyanophage in China. *PNAS* 2002; 12:923-927.

Zhu W, Sun Q, Chen F, Li M. Cellular N:P ratio of *Microcystis* as an indicator of nutrient limitation – implications and applications. *Environmental Earth Sciences* 2015; 74:4023-4030.

